RESEARCH MEMORANDUM

EFFECT OF FREE-STREAM MACH NUMBER ON GROSS-FORCE AND PUMPING CHARACTERISTICS OF SEVERAL EJECTORS

By Leonard E. Stitt and Alfred S. Valerino

Lewis Flight Propulsion Laboratory
Cleveland, Ohio

NATIONAL ADVISORY COMMITTEE
FOR AERONAUTICS

WASHINGTON

March 15, 1955
Declassified December 3, 1958

NATIONAL ADVISORY COMMITTEE FOR AERONAUTICS

RESEARCH MEMORANDUM

EFFECT OF FREE-STREAM MACH NUMBER ON GROSS-FORCE AND PUMPING CHARACTERISTICS OF SEVERAL EJECTORS

By Leonard E. Stitt and Alfred S. Valerino

SUMMARY

An investigation was conducted in the 8- by 6-foot supersonic wind tunnel to determine the effects of free-stream Mach number on the gross-force and pumping characteristics of several ejectors. This investigation was conducted at free-stream Mach numbers of 0.10, 0.63, and 1.50 and in quiescent air over a primary-nozzle pressure-ratio range of 2 to 10, secondary-to-primary weight-flow ratios to 0.43, and at primary gas temperatures from 540° to 2000° R.

Results of this investigation indicated that both ejector gross force and secondary-to-primary total-pressure ratio were reduced when the external stream was changed from subsonic to a supersonic value of 1.50 as a result of overexpansion of the primary jet associated with off-design operation of these ejectors. The magnitude of this effect was reduced by increasing both pressure ratio and secondary weight flow.

INTRODUCTION

Many experimental investigations have been conducted to evaluate ejector performance (refs. 1 to 4); however, the majority of these data are limited to tests in quiescent air and do not include any information on the effect of the external stream. Therefore, the NACA Lewis laboratory is conducting a program to determine the effects of free-stream Mach number on both ejector gross-force and pumping characteristics.

The gross-force and pumping characteristics of a series of ejectors, suitable for installation on a proposed supersonic aircraft, have been presented in reference 5 with the primary nozzle in the simulated afterburner-on position. The tests were conducted at free-stream Mach numbers from 0.1 to 1.9 over a range of primary pressure ratio and secondary weight flow. Results of this investigation indicated that free-stream Mach number had no effect on the gross-force and pumping characteristics of the ejectors. However, the range of diameter ratio

D_s/D_p for these ejectors was sufficiently low that the primary jet was not greatly overexpanded and that the secondary flow choked over the pressure-ratio range investigated at supersonic free-stream conditions.

In the present report, with the primary nozzle in the afterburner-off position, the resulting diameter ratios are of such order that the primary jet would be greatly overexpanded if it filled the secondary passage and that the secondary flow, in most cases, would be unchoked over the pressure-ratio range investigated. The tests were conducted at free-stream Mach numbers from zero to 1.5 over a range of primary pressure ratio and secondary weight flow. At subsonic speeds, the data are representative of realistic operating conditions of the fixed-shroud ejector. However, at supersonic speeds, the nozzle would usually conform to the afterburner-on condition (ref. 5). The data presented herein at supersonic speeds, however, assume physical significance if afterburner-off deceleration is being considered. In addition, these data may be applied to the problem of ejector nozzles designed for Mach numbers greater than 1.5, but operating at lower supersonic speeds without geometry changes.

SYMBOLS

The following symbols are used in this report and some are shown in the following sketch:

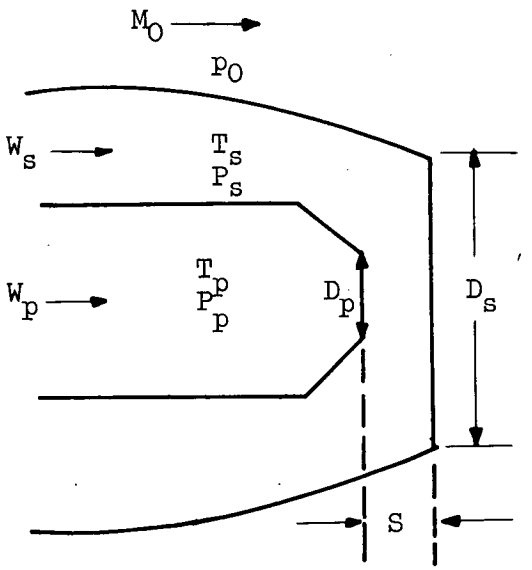

A	area, sq in.
C_F	thrust coefficient, ratio of measured jet thrust to thrust available with isentropic flow in convergent nozzle
C_f	discharge coefficient, ratio of measured mass flow to isentropic mass flow
D	exit diameter, in.
D_s/D_p	diameter ratio
F_e	gross force, lb
F_j	jet thrust, lb
M	Mach number
P	total pressure, lb/sq ft
p	static pressure, lb/sq ft
S	spacing, distance from primary exit to shroud exit, in.
S/D_p	spacing ratio
T	total temperature, $^{\circ}R$
W	weight flow, lb/sec
$\frac{W_s}{W_p}\sqrt{\frac{T_s}{T_p}}$	corrected weight-flow ratio
γ	ratio of specific heats

Subscripts:

e	ejector
j	jet
p	primary nozzle
s	secondary shroud
0	free stream

APPARATUS AND PROCEDURE

Installation

A schematic diagram and a photograph of the exit model installed in the 8- by 6-foot supersonic wind tunnel are presented in figures 1(a) and (b), respectively. Air, which was preheated to 250° F, was introduced into the model through two hollow support struts. A detailed discussion of the general model installation in the tunnel is presented in reference 6.

The quiescent-air test rig was located in the lower balance chamber of the 8- by 6-foot tunnel. The primary-nozzle pressure-ratio range was obtained by supplying the model with high-pressure air as described in reference 6 and by lowering the ambient pressure of the balance chamber by means of exhausters. A photograph of the quiescent-air test rig is presented in figure 2.

A schematic diagram of the model showing pertinent external model stations and internal details is presented in figure 3. The external shrouds investigated were mounted at station 70.61. The collar shown simulated the mechanism for varying the nozzle-throat area.

Ejector Configurations

Sketches and pertinent dimensions of the ejectors investigated are presented in figure 4 together with tables of the internal contour coordinates of the shrouds. The primary nozzle, which was the same for all the shroud configurations investigated, had a throat diameter of 2.82 inches, simulating the afterburner-off case.

The ejector configurations are designated by two numbers: the first number designates diameter ratio, and the second number designates spacing ratio. For example, the basic configuration (1.97-0) had a diameter ratio D_s/D_p of 1.97 and a spacing ratio S/D_p of zero.

Ejectors 1.72-0.76 and 1.97-0 were obtained by cutting back the shroud of ejector 1.54-1.11. In this manner, the diameter ratio increased as the spacing ratio decreased. Ejector 1.54-0.55 had the same diameter ratio as ejector 1.54-1.11; however, the spacing was reduced approximately one-half resulting in a larger boattail angle. Ejector 1.54-1.11S was identical to ejector 1.54-1.11 except that simulated stiffener rings were installed on the inside of the shroud as shown in figure 4(e).

Data Reduction

The method of force measurements and the reduction of these data are described in detail in reference 5. Total weight flow to the model was obtained from the sharp-edged orifice shown in figure 1(a) and from rotameters that measured preheater and main combustor fuel flow. Primary-nozzle weight flow W_p was then calculated by subtracting the calibrated secondary weight flow W_s from the total weight flow. Primary-nozzle total pressure P_p was obtained from a static pressure measured at model station 70.16 and the calibrated value of discharge coefficient C_f. Primary-nozzle total temperature T_p was then obtained from continuity relations where total pressure, weight flow, and discharge coefficient were known.

RESULTS AND DISCUSSION

Effect of Heat Addition on Primary-Nozzle Performance

The calibrated jet thrust of the primary nozzle alone, with and without heat addition, is presented in figure 5. Part of these data were obtained in quiescent air and part in the wind tunnel. The calculated thrust of an ideal convergent nozzle is also presented in figure 5 to compare with the measured thrusts. This ideal thrust was computed by assuming a ratio of specific heats γ of 1.40 and a nozzle discharge coefficient C_f of 1.0. The difference between the measured and calculated jet thrust of the primary nozzle without heat addition (fig. 5(a)) can be accounted for by the 0.94 value of discharge coefficient that was obtained for this nozzle over the range of primary pressure and weight-flow ratios investigated (fig. 6). The indicated $5\frac{1}{2}$-percent decrease in jet thrust between the cold- and hot-flow data (fig. 5(b)) is not believed to be physically realistic; the decrease probably resulted primarily from plotting the measured thrust data at calculated values of pressure ratio P_p/p_0 higher than those actually existing at the nozzle-exit station. This error in pressure ratio is presumed to arise from the method of computing primary-nozzle total pressure P_p. As was explained in APPARATUS AND PROCEDURE, nozzle total pressure was computed on the basis of the measured static pressure at the nozzle entrance and would not include any loss in total pressure arising from delayed combustion between this station and the nozzle-exit station. However, small decreases in thrust may have occurred from combustion-induced nonuniform velocity profiles in the primary stream and from changes in gas specific heats associated with the change in gas temperature and chemical composition.

Effect of Heat Addition on Ejector Jet Thrust

The difference in ejector jet thrust with and without heat addition (fig. 7) was of the same order as the difference in primary-nozzle jet thrust (fig. 5(b)). Therefore, the ratios of ejector to primary-nozzle jet thrust with and without heat addition (fig. 8) were nearly identical. Data are presented for only one ejector; however, similar results were obtained for several of the other ejectors investigated. The ratio of secondary to primary total pressure P_s/P_p was essentially unaffected by the addition of heat, as is also illustrated in figure 8. The remaining data in this report were obtained with heat addition, so the ejector forces are presented in terms of the calibrated jet thrust $F_{j,p}$ obtained with heat addition.

Effect of Free-Stream Mach Number on Ejector Performance

Without secondary flow. - Only the configuration having zero shroud length (1.97-0) was investigated with no secondary flow. This configuration was equivalent to a convergent nozzle surrounded by a blunt annular base. Small-scale investigations of jet effects on the base pressures of such nozzle-body combinations have been reported in references 7 and 8 for subsonic and supersonic speeds, respectively. The values reported herein (fig. 9) are in general agreement with those of the referenced reports, as indicated by the estimated base pressures. In making the estimates, it was necessary to extrapolate the data at supersonic speeds to a Mach number of 1.50. No correction was made to account for the differences in boattail profile. For the subsonic case, base pressures at a Mach number of 0.90 were assumed equal to those at 0.63. At subsonic speeds, the jet aspirated the annular base pressure slightly below ambient pressure for the range of primary-nozzle pressure ratio considered. At a Mach number of 1.50, the base pressures were below the no-jet value for the pressure-ratio range covered and increased with increasing values of pressure ratio as discussed in reference 8. The jet thrust values were unaffected by the external stream.

With secondary flow. - The experimental pumping and gross force data obtained in the wind tunnel for the five ejector configurations with secondary flow are presented in figures 10 to 12 for free-stream Mach numbers of 0.10, 0.63, and 1.50, respectively. The gross ejector force F_e for any configuration consists of its jet thrust minus external drag plus the jet-off drag of the basic configuration (1.97-0). Thus, the gross ejector force for any given configuration consists of its jet thrust, the change in external drag due to the jet exhaust, and any difference in jet-off external drag between it and the basic configuration. Such a parameter permits a comparison of the configurations on an over-all basis.

Cross plots of these data together with data obtained in quiescent air are presented in figure 13 for three configurations to illustrate the free-stream effect with secondary flow. It should be pointed out that data points are shown only to distinguish between free-stream Mach number since the curves represent interpolated values.

Both ejector gross-force ratio and secondary-to-primary total-pressure ratio were consistently lower for Mach number 1.50 than for quiescent air for all configurations. The decrease in ejector gross force at Mach number 1.50 was caused by the reduction of pressure at the exit of the secondary passage associated with a supersonic stream and by overexpansion of the primary jet resulting from off-design operation of these ejectors. The total-pressure ratio was lower at a Mach number of 1.50 even when the secondary-flow passage was choked; that is, when the secondary-to-primary total-pressure ratio remained constant with increasing values of primary-nozzle pressure ratio. A possible explanation for this phenomenon can be seen by referring to the static-pressure plot and the sketch in figure 9. For a given primary-nozzle pressure ratio, the local static pressure in region 2 is lower for a supersonic stream than in quiescent air or a subsonic stream because of the expansion around the shroud exit. Thus, for choking of the secondary passage ($P_s/p_2 = 1.893$), the level of P_s would depend on the level of p_2 and would therefore be lower for the case of a supersonic stream than for the case with quiescent air.

Ejector Characteristics

Ejector characteristics for all five configurations investigated are presented in figure 14 to illustrate the effect of primary-nozzle pressure ratio on gross force and secondary-to-primary total-pressure ratio for constant values of secondary weight-flow ratio. A comparison of the gross-force and pumping characteristics for Mach numbers of 0.10 and 0.63 suggests the possibility of a Mach number effect, although the magnitude of the effect is small compared with that at a Mach number of 1.50.

The relatively large thrust losses at a primary-nozzle pressure ratio of 2.0 and low weight-flow ratios probably resulted from overexpansion of the primary stream, as was discussed in reference 1. As pointed out in references 1, 9, and 10, this effect was lessened by the addition of secondary weight flow. It is also apparent that the addition of secondary flow lessened the effect of the external supersonic stream.

A comparison of figures 14(d) and (e) indicates the effect on ejector performance of adding stiffener rings on the inside of the exit shroud. There is essentially no effect on pumping characteristics, as

was also concluded in reference 5. The ejector gross-force ratios were nearly equal for Mach numbers of 0.10 and 0.63, but the stiffener rings caused a reduction in gross force at a Mach number of 1.50, particularly at the higher values of primary-nozzle pressure ratio where the jet probably interacted with the rings. The results of reference 5 indicated that, for the simulated afterburner-on condition, addition of stiffener rings had no effect on gross force.

Effect of Cutting Back the Shroud on Ejector Performance

As shown by the sketch in figure 15, ejector 1.72-0.76 and 1.97-0 resulted from cutting back the shroud of ejector 1.54-1.11 along its contour. In this manner, the diameter ratio increased as the spacing ratio decreased. The ejector gross-force data, obtained from cross plots of figure 14, are presented for a low and high value of primary-nozzle pressure ratio at constant values of weight-flow ratio.

For primary pressure ratios of 3.0 and 7.0, the point of optimum gross force shifted to a lower value of spacing ratio as weight-flow ratio increased; however, for comparable values of weight-flow ratio, the optimum point shifted to a higher value of spacing ratio as primary-nozzle pressure ratio increased.

For a primary-nozzle pressure ratio of 3.0 (fig. 16(a)), cutting back the shroud has little effect on pumping except at the higher values of secondary weight flow. For weight-flow ratios of 0.25 and 0.35, the pumping is optimum for values of spacing ratio of 0.5 and 0.6, respectively. For a primary-nozzle pressure ratio of 7.0 (fig. 16(b)), the pumping is optimum for values of spacing ratio between 0.20 and 0.60, depending on weight-flow ratio. The shift of the optimum point to higher values of spacing ratio with increases in weight-flow ratio is evident at both values of primary-nozzle pressure ratio.

The results of figures 15 and 16 indicate that, from both a gross force and pumping consideration, ejector 1.72-0.76 would generally be superior to ejectors 1.54-1.11 and 1.97-0. This was true for both the realistic subsonic case and the off-design case at a Mach number of 1.50 where the diameter ratios of these ejectors were too large for the available primary-nozzle pressure ratios. It is interesting to note that in the afterburner-on condition (ref. 5) this same ejector shroud proved to be one of the optimum configurations.

Effect of Spacing Ratio on Ejector Performance

As shown on the sketch in figure 17, ejector 1.54-0.55 had the same diameter ratio as ejector 1.54-1.11, but the spacing was reduced approximately one-half by boattailing. For a primary-nozzle pressure ratio of

3.0 (fig. 17(a)), optimum gross force would be obtained for a spacing ratio less than 0.55. At a primary-nozzle pressure ratio of 7.0, the optimum gross force occurs at a spacing ratio greater than 1.11. For the two configurations investigated, spacing ratio had little effect on the pumping characteristics, as illustrated in figure 18.

A comparison of results between figures 18 and 16 would indicate that diameter ratio has more effect on pumping than spacing ratio. This conclusion was also pointed out in the results of reference 5, for example.

SUMMARY OF RESULTS

The following results were obtained from an investigation of several ejectors with the primary nozzle in the simulated afterburner-off position. The investigation was conducted at free-stream Mach numbers of 0.10, 0.63, and 1.50 and in quiescent air over a range of primary-nozzle pressure ratio and secondary weight flow at primary gas temperatures from 540° to 2000° R.

1. At a given value of primary-nozzle pressure ratio and secondary weight-flow ratio, both ejector gross force and secondary-to-primary total-pressure ratio decreased when the free-stream Mach number was changed from a subsonic value to a supersonic value of 1.50. This decrease resulted from overexpansion of the primary jet associated with off-design operation of these ejectors. This Mach number effect decreased with increasing values of both primary-nozzle pressure ratio and secondary weight flow.

2. Of all the configurations investigated, ejector 1.72-0.76 appeared to be the best from both a gross-force and a pumping standpoint. This was true both subsonically and at off-design operation at a Mach number of 1.50.

Lewis Flight Propulsion Laboratory
National Advisory Committee for Aeronautics
Cleveland, Ohio, December 1, 1954

REFERENCES

1. Greathouse, W. K.: Preliminary Investigation of Pumping and Thrust Characteristics of Full-Size Cooling Air-Ejectors at Several Exhaust-Gas Temperatures. NACA RM E54A18, 1954.

2. Greathouse, W. K., and Hollister, D. P.: Preliminary Air-Flow and Thrust Calibrations of Several Conical Cooling-Air Ejectors with a Primary to Secondary Temperature Ratio of 1.0. I - Diameter Ratios of 1.21 and 1.10. NACA RM E52E21, 1952.

3. Greathouse, W. K., and Hollister, D. P.: Preliminary Air-Flow and Thrust Calibrations of Several Conical Cooling-Air Ejectors with a Primary to Secondary Temperature Ratio of 1.0. II - Diameter Ratios of 1.06 and 1.40. NACA RM E52F26, 1952.

4. Huntley, S. C., and Yanowitz, Herbert: Pumping and Thrust Characteristics of Several Divergent Cooling-Air Ejectors and Comparison of Performance with Conical and Cylindrical Ejectors. NACA RM E53J13, 1954.

5. Hearth, Donald P., and Valerino, Alfred S.: Thrust and Pumping Characteristics of a Series of Ejector-Type Exhaust Nozzles at Subsonic and Supersonic Flight Speeds. NACA RM E54H19, 1954.

6. Hearth, Donald P., and Gorton, Gerald C.: Investigation of Thrust and Drag Characteristics of a Plug-Type Exhaust Nozzle. NACA RM E53L16, 1954.

7. Salmi, Reino J.: Experimental Investigation of Drag of Afterbodies with Exiting Jet at High Subsonic Mach Numbers. NACA RM E54I13, 1954.

8. Cortright, Edgar M., Jr., and Kochendorfer, Fred D.: Jet Effects on Flow over Afterbodies in Supersonic Stream. NACA RM E53H25, 1953.

9. Vargo, Donald J.: Effects of Secondary-Air Flow on Annular Base Force of a Supersonic Airplane. NACA RM E54G28, 1954.

10. O'Donnell, Robert M., and McDearmon, Russell W.: Experimental Investigation of Effects of Primary Jet Flow and Secondary Flow Through a Zero-Length Ejector on Base and Boattail Pressures of a Body of Revolution at Free-Stream Mach Numbers of 1.62, 1.93, and 2.41. NACA RM L54I22, 1954.

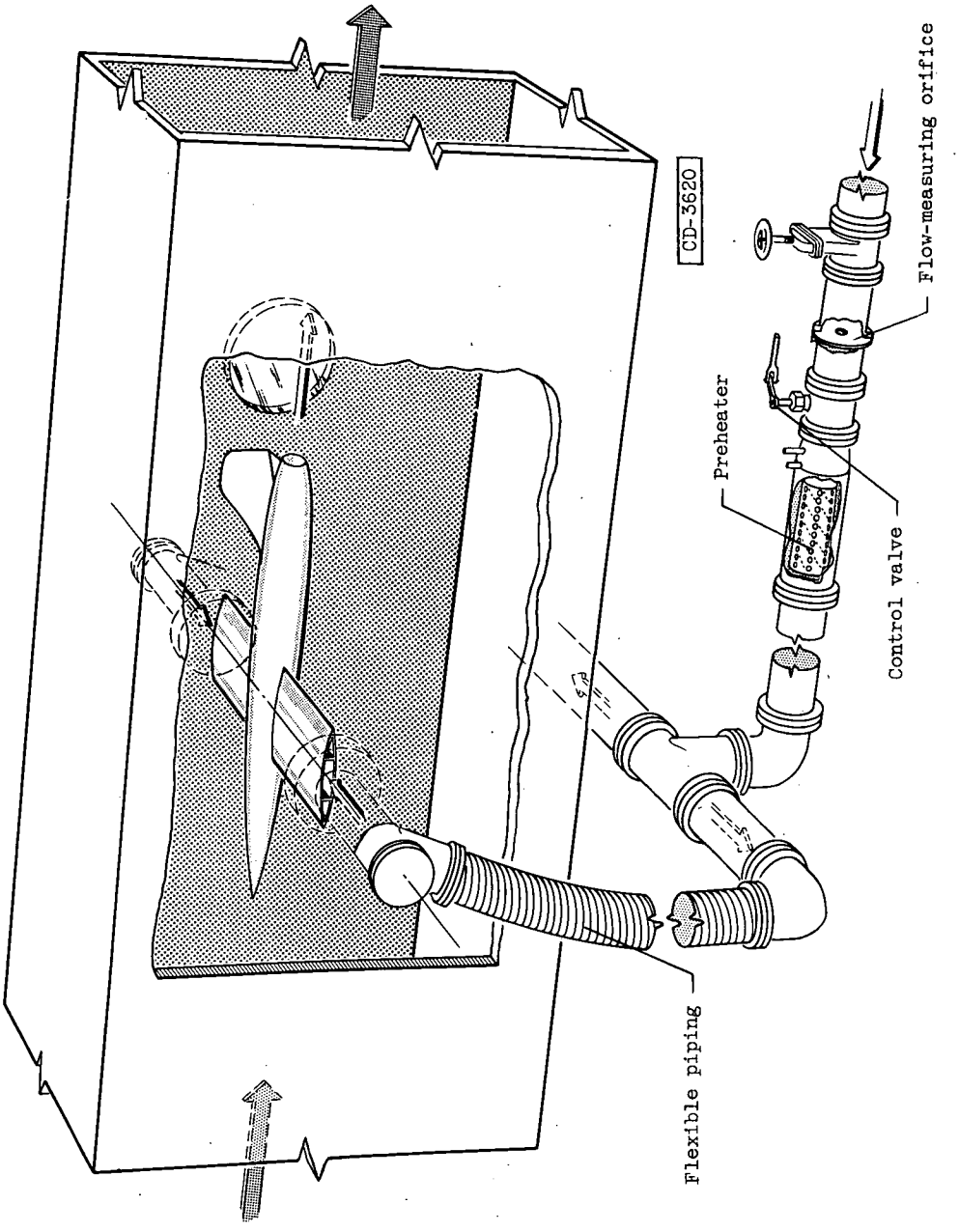

(a) Schematic diagram.

Figure 1. - Model installation in 8- by 6-foot supersonic wind tunnel.

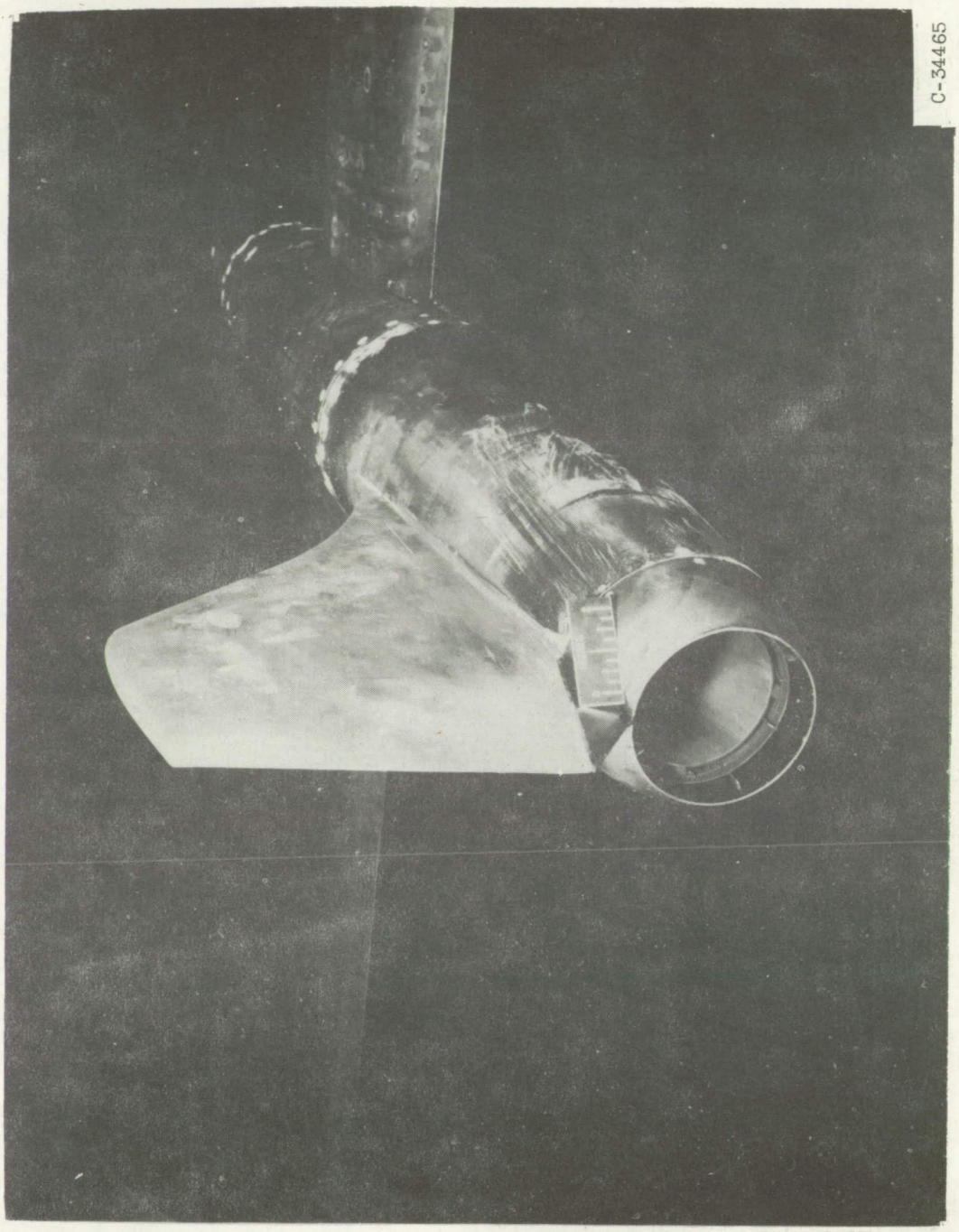

(b) Photograph.

Figure 1. - Concluded. Model installation in 8-by 6-foot supersonic wind tunnel.

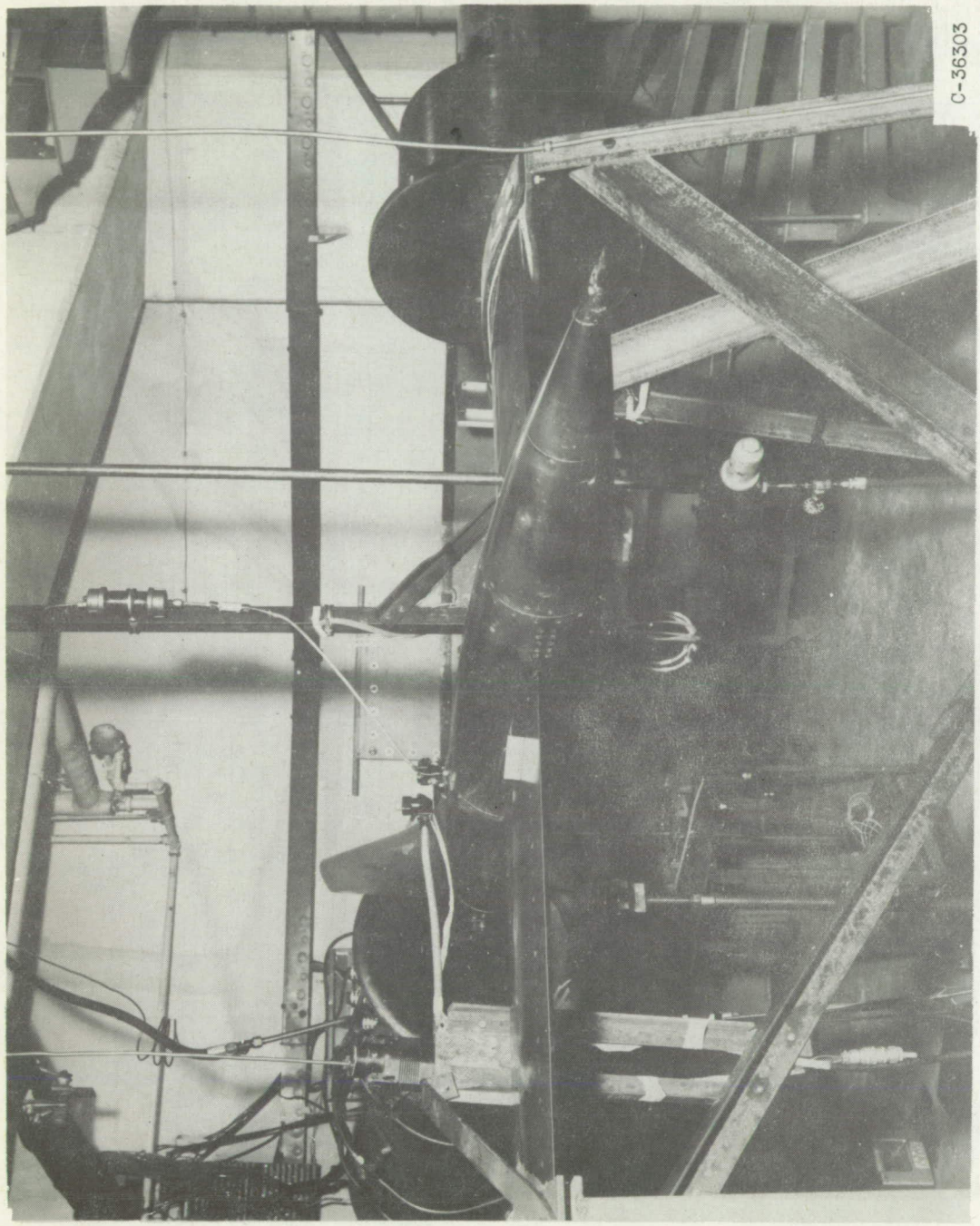

Figure 2. - Quiescent-air test rig.

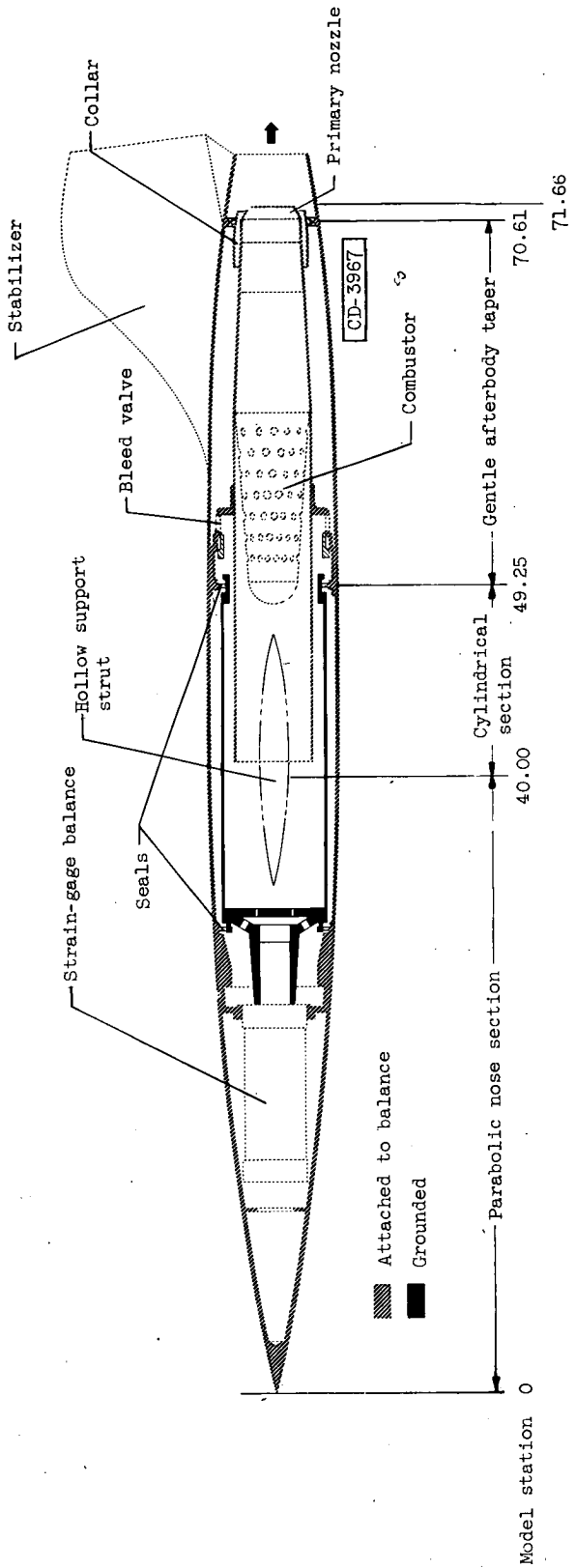

Figure 3. - Schematic diagram of model (all dimensions in inches).

Shroud internal contour	
Fuselage station	Inside diameter
70.61	5.74
71.66	5.55

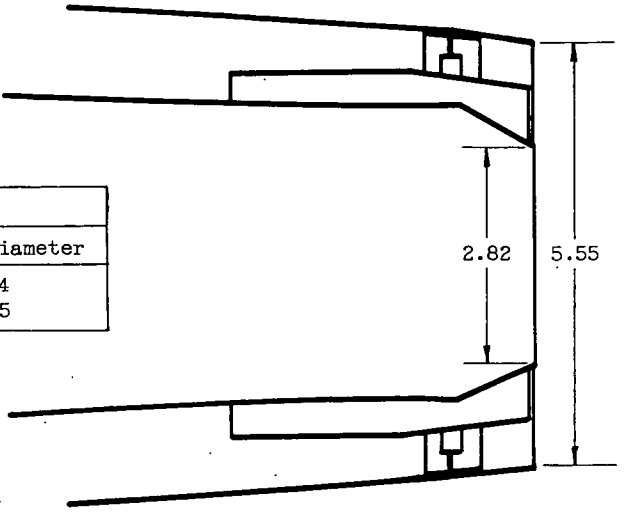

(a) Ejector 1.97-0.

Shroud internal contour	
Fuselage station	Inside diameter
70.61	5.74
71.15	5.63
71.66	5.43
72.20	5.15
72.72	4.75
73.18	4.34

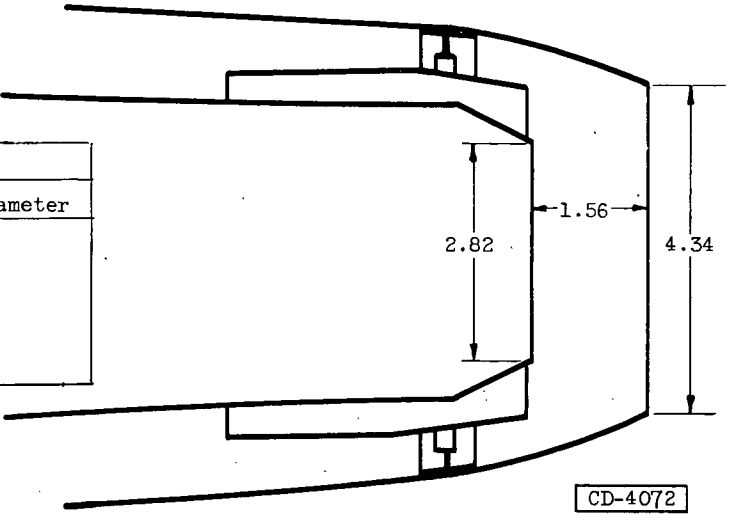

(b) Ejector 1.54-0.55.

Figure 4. - Ejector configurations (all dimensions in inches).

Shroud internal contour	
Fuselage station	Inside diameter
70.61	5.74
71.66	5.55
72.72	5.26
73.77	4.86

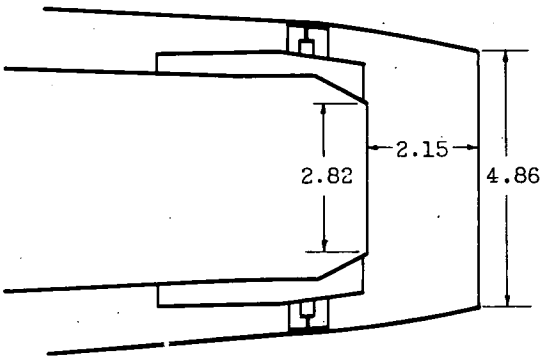

(c) Ejector 1.72-0.76.

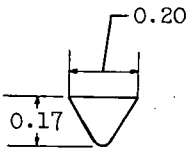

Enlarged view of stiffener ring

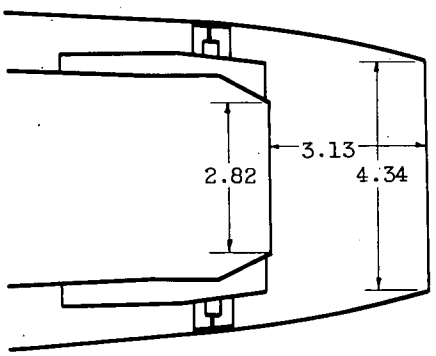

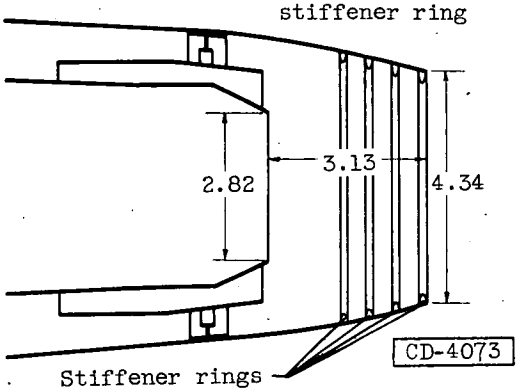

Shroud internal contour	
Fuselage station	Inside diameter
70.61	5.74
71.66	5.55
72.72	5.26
73.77	4.86
74.75	4.34

(d) Ejector 1.54-1.11.

Shroud internal contour	
Fuselage station	Inside diameter
70.61	5.74
71.66	5.55
72.72	5.26
73.77	4.86
74.75	4.34

(e) Ejector 1.54-1.11S.

Figure 4. - Concluded. Ejector configurations (all dimensions in inches).

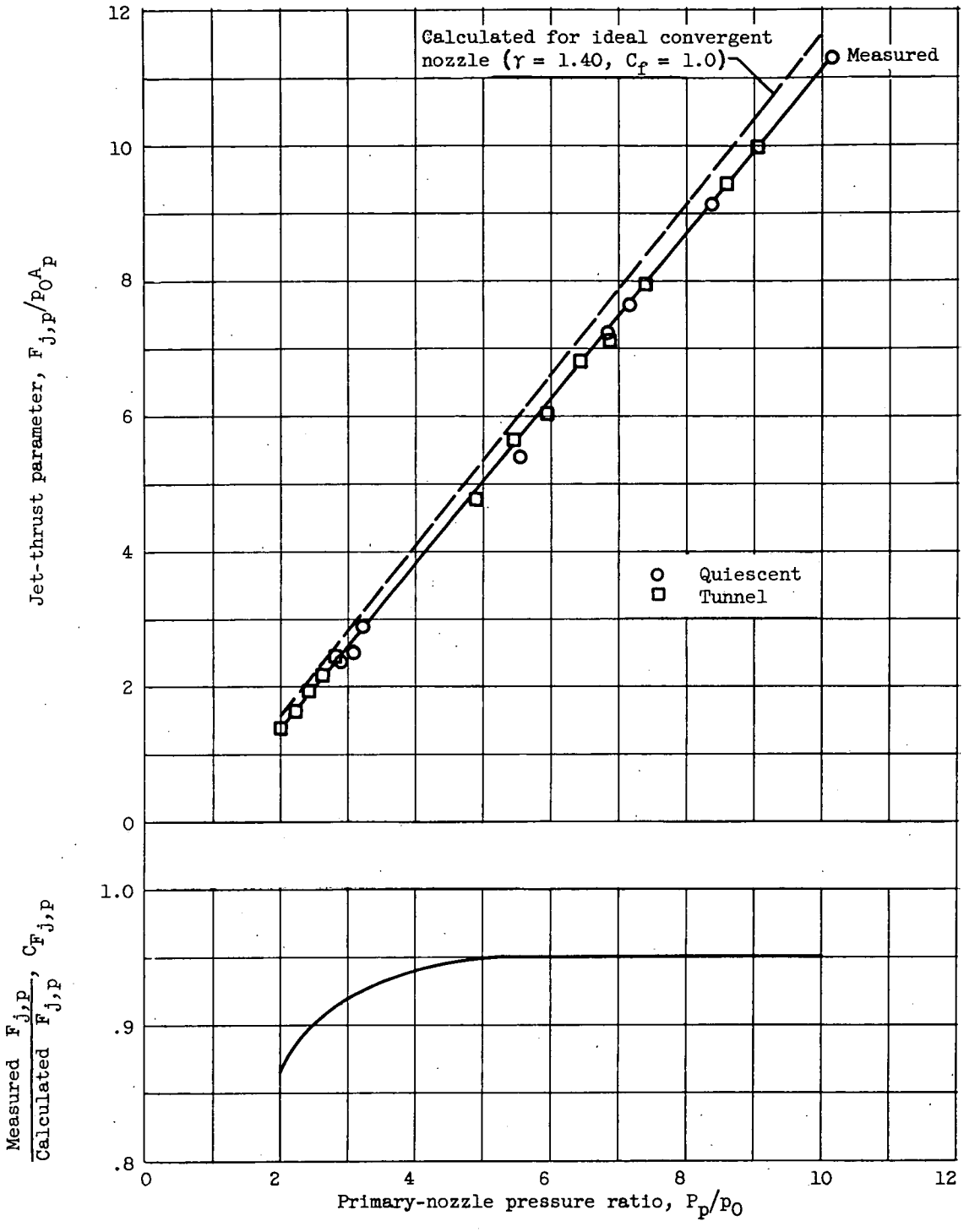

(a) Primary gas temperature, T_p, 540° R.

Figure 5. - Jet-thrust performance of 2.82-inch-diameter conical primary nozzle.

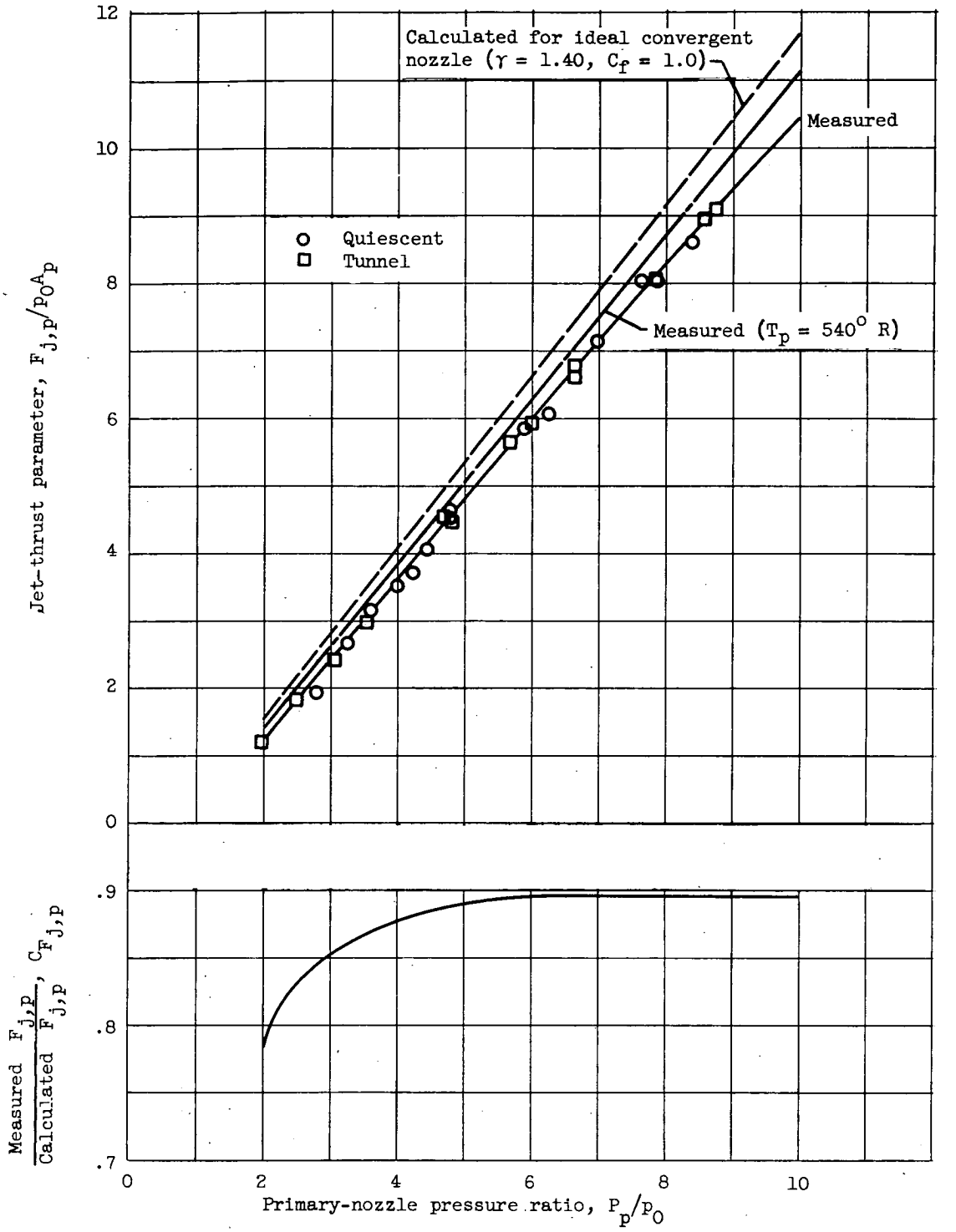

(b) Primary gas temperature, T_p, 1000° to 2000° R.

Figure 5. - Concluded. Jet-thrust performance of 2.82-inch-diameter conical primary nozzle.

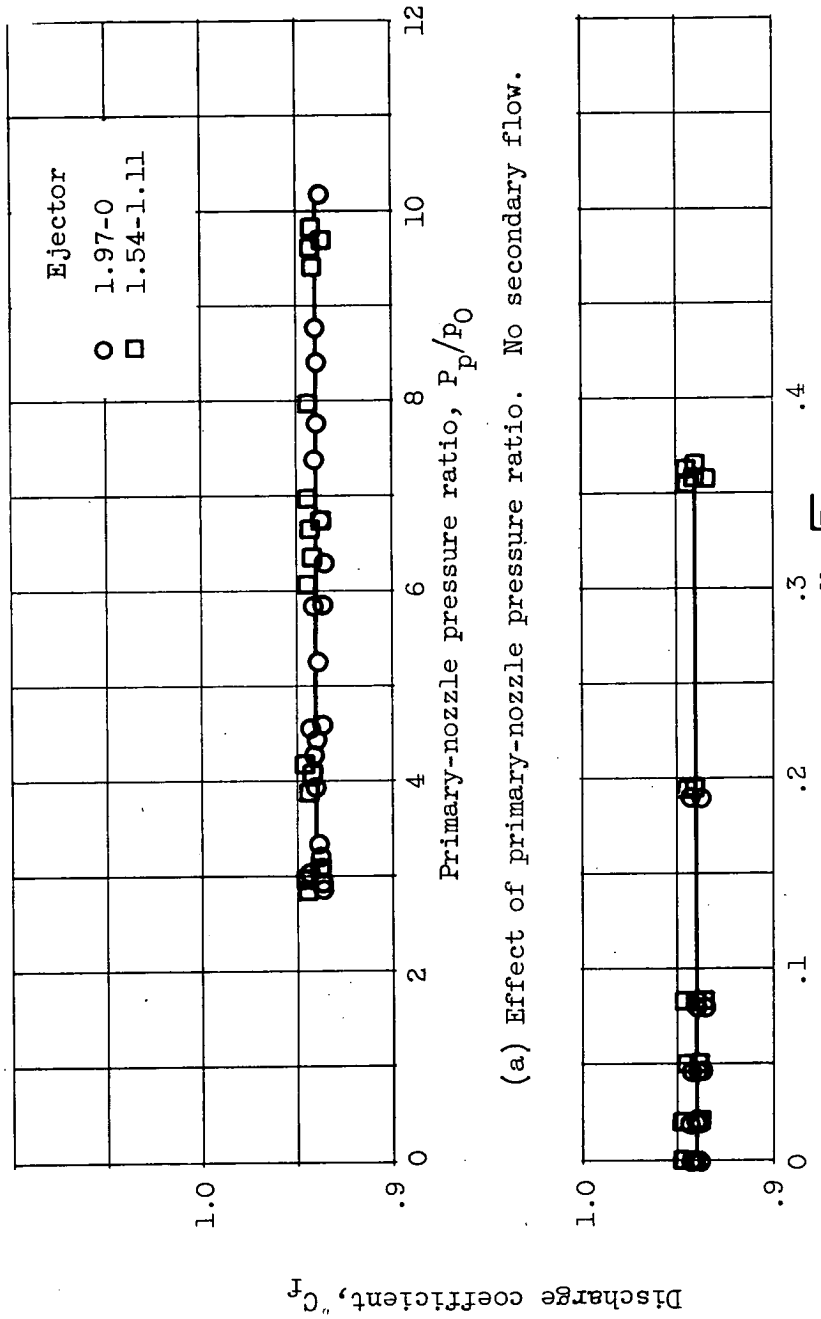

Figure 6. - Primary-nozzle discharge coefficient. Primary gas temperature, 540° R.

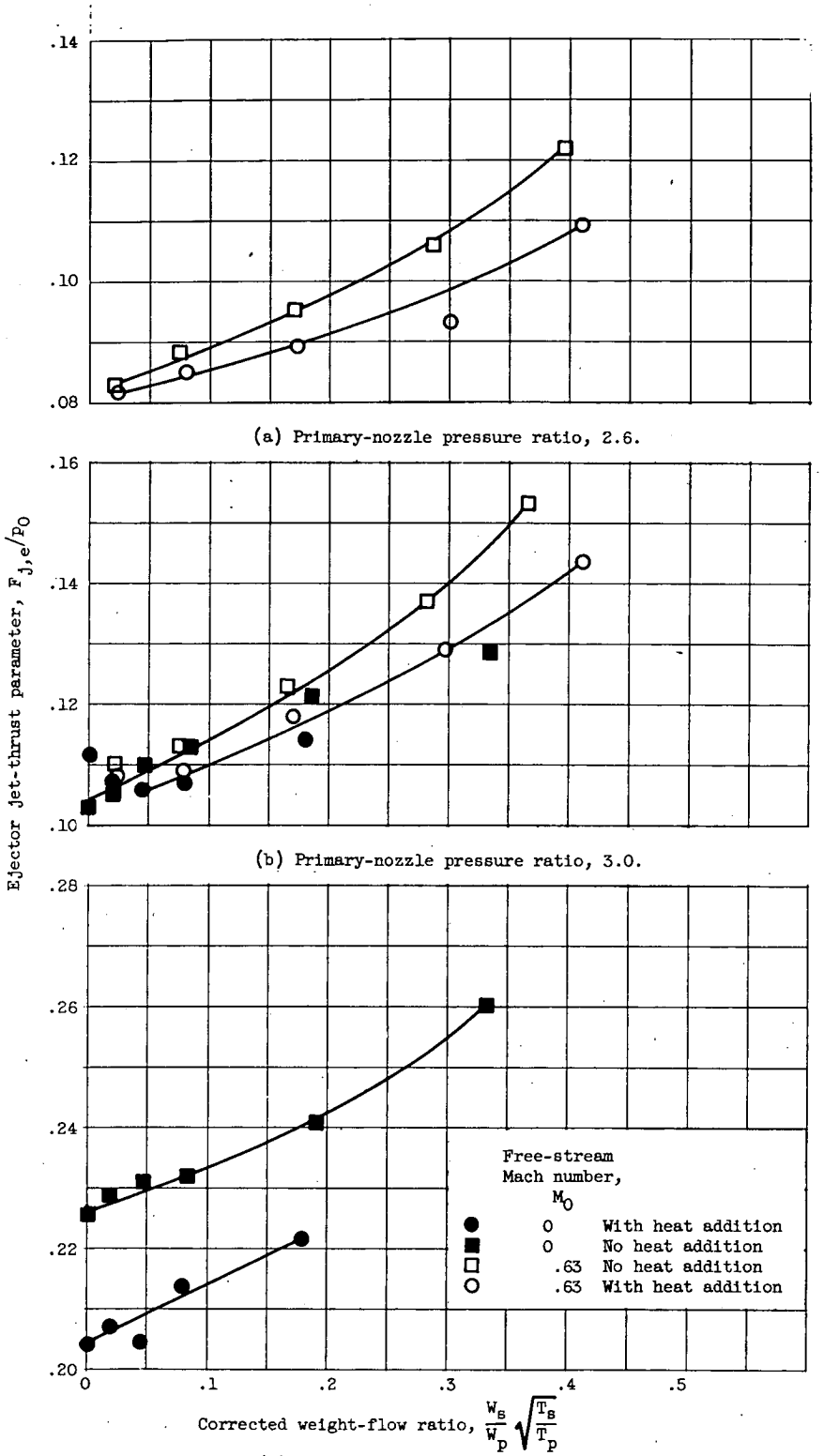

Figure 7. - Effect of heat addition on jet thrust of ejector 1.54-1.11S.

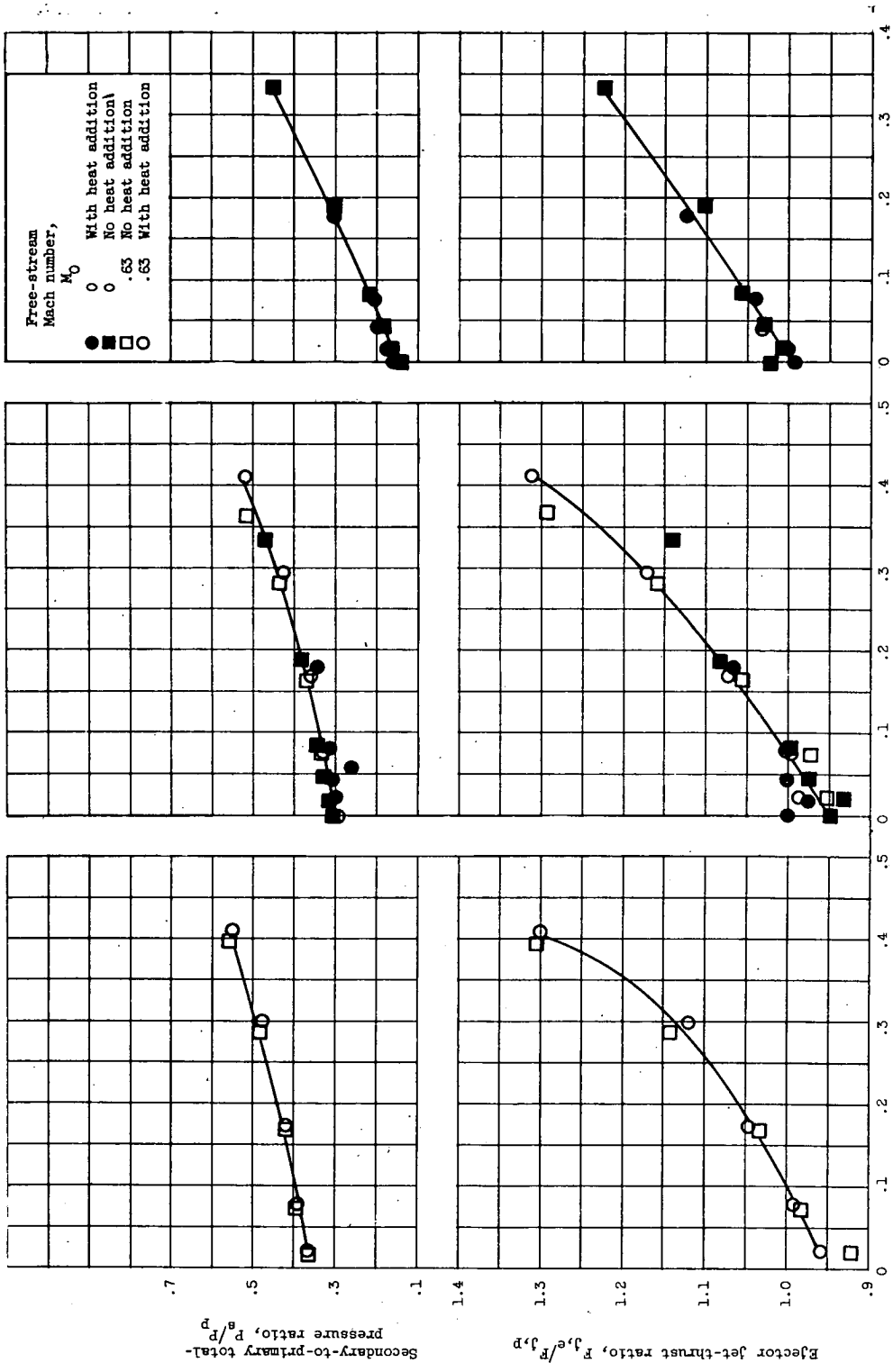

(a) Primary-nozzle pressure ratio, 2.6. (b) Primary-nozzle pressure ratio, 3.0. (c) Primary-nozzle pressure ratio, 5.0.

Figure 8. - Effect of heat addition on jet-thrust ratio and pumping characteristics of ejector 1.54-1.11S.

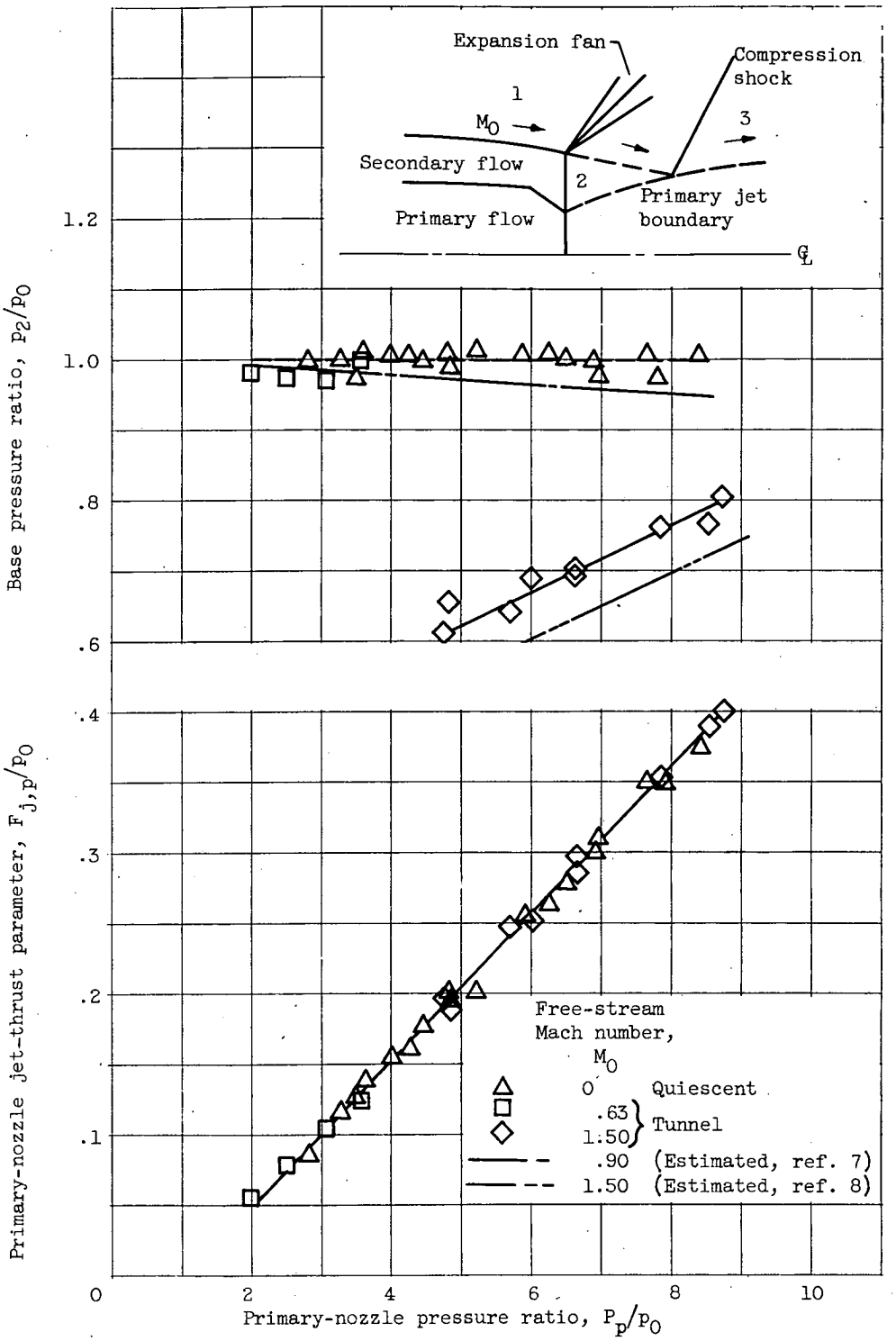

Figure 9. - Effect of free-stream Mach number on primary-nozzle jet thrust and base pressure of ejector 1.97-0. No secondary flow.

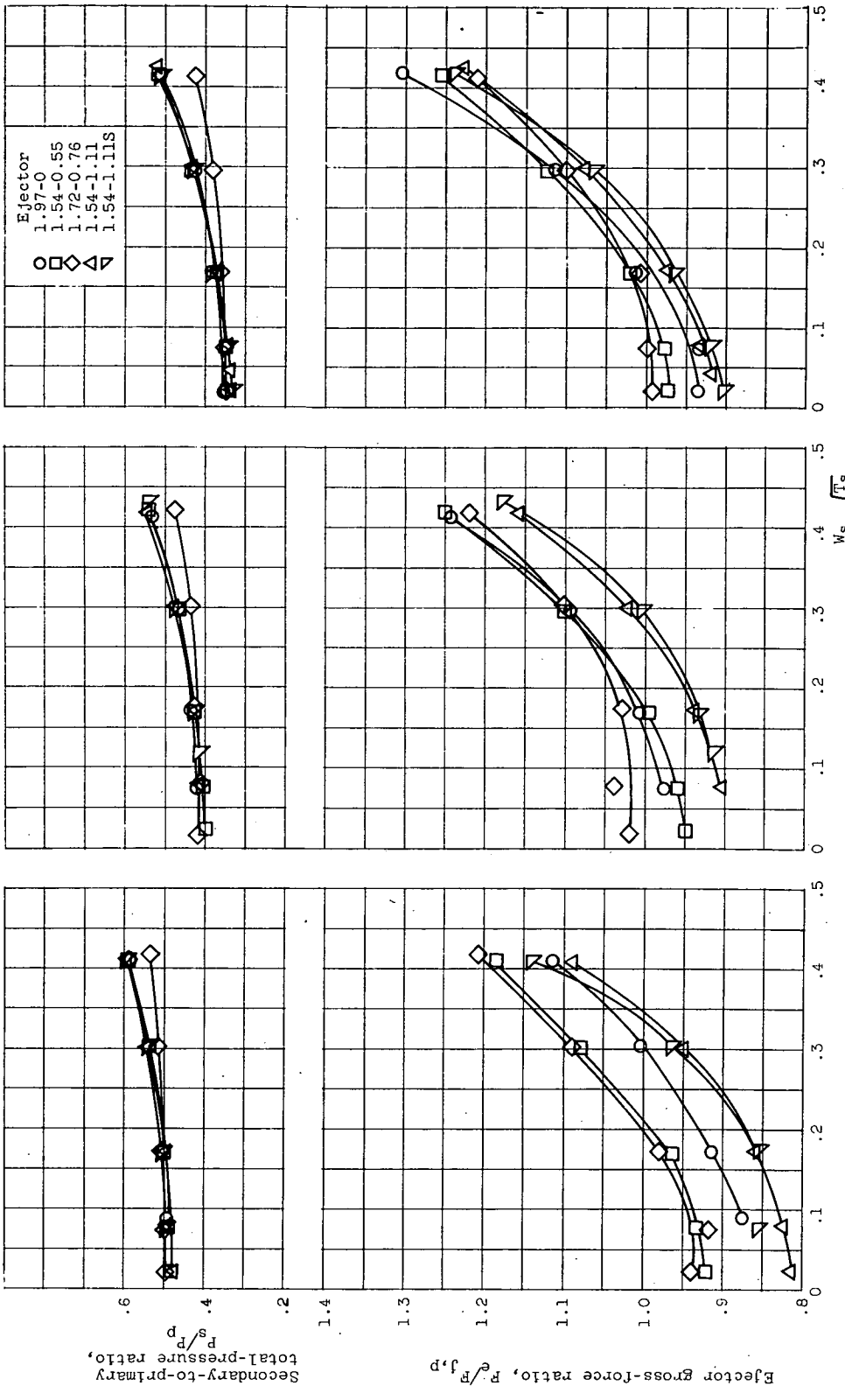

(a) Primary-nozzle pressure ratio, 2.00. (b) Primary-nozzle pressure ratio, 2.45. (c) Primary-nozzle pressure ratio, 2.85.

Figure 10. - Ejector pumping and gross-force characteristics. Free-stream Mach number, 0.10.

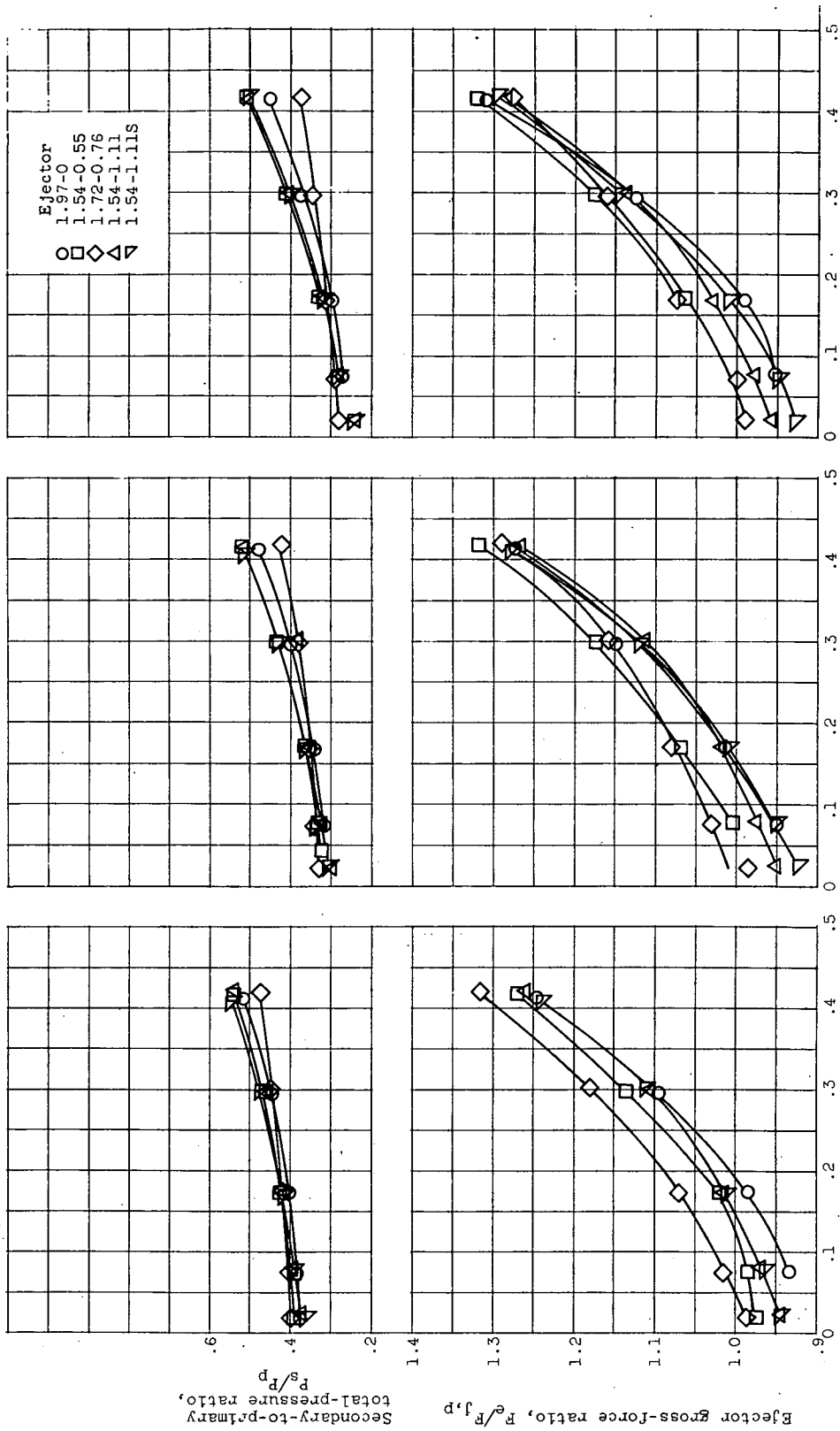

Figure 11. - Ejector pumping and gross-force characteristics. Free-stream Mach number, 0.63.

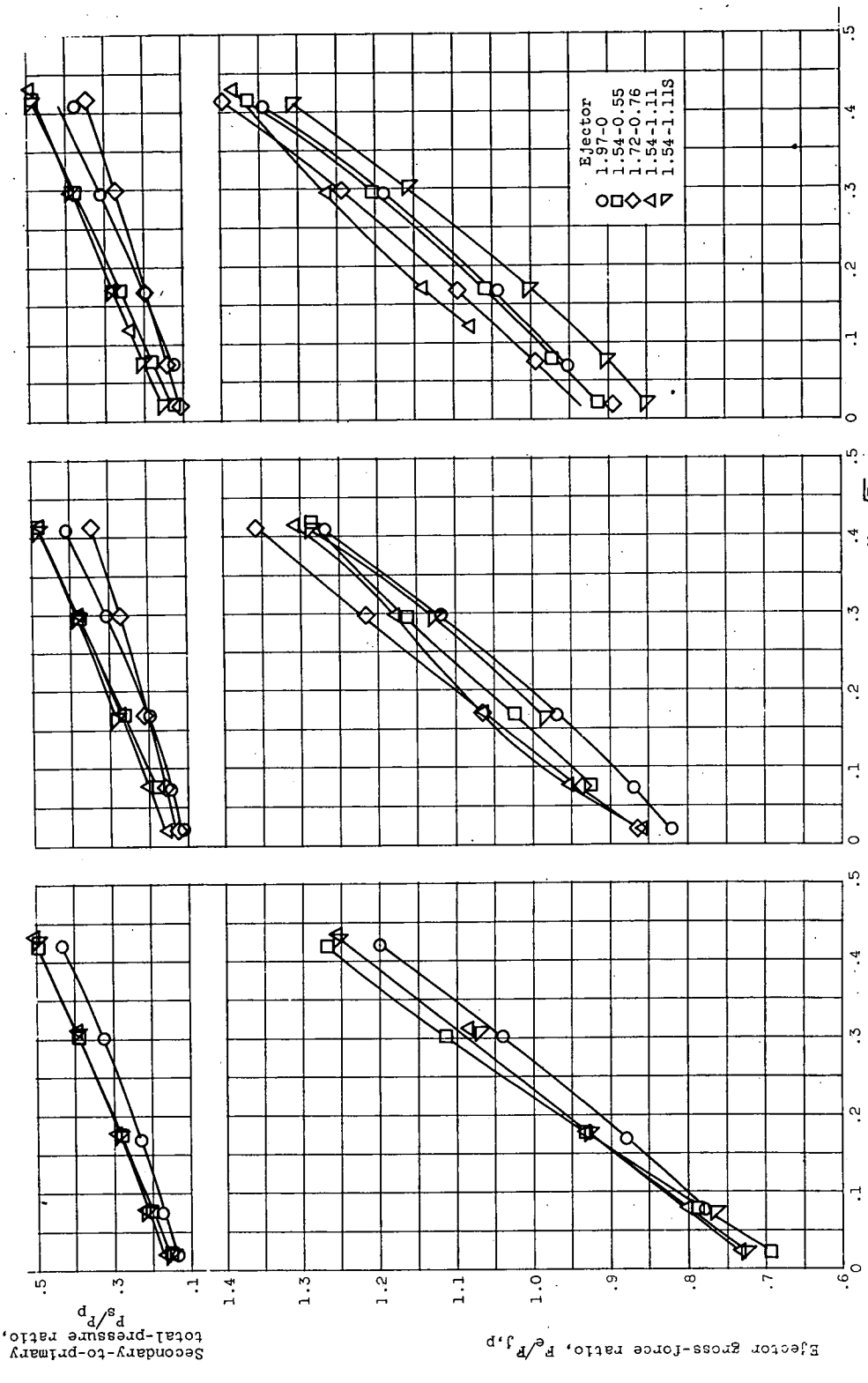

(a) Primary-nozzle pressure ratio, 4.85. (b) Primary-nozzle pressure ratio, 6.90. (c) Primary-nozzle pressure ratio, 8.75.

Figure 12. - Ejector pumping and gross-force characteristics. Free-stream Mach number, 1.50.

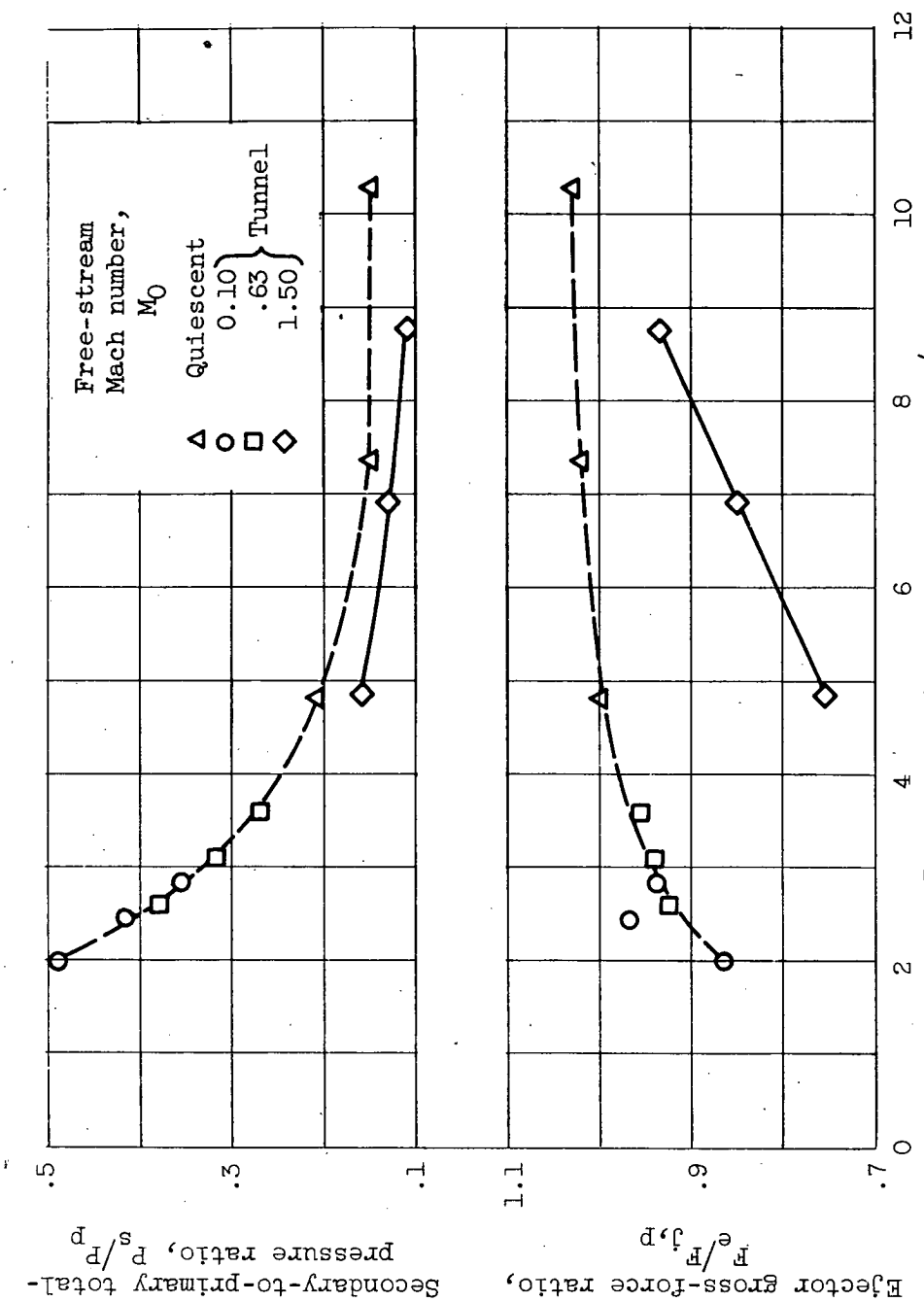

(a) Ejector 1.97-0.

Figure 13. - Comparison of quiescent-air and tunnel experimental data. Corrected weight-flow ratio, 0.05.

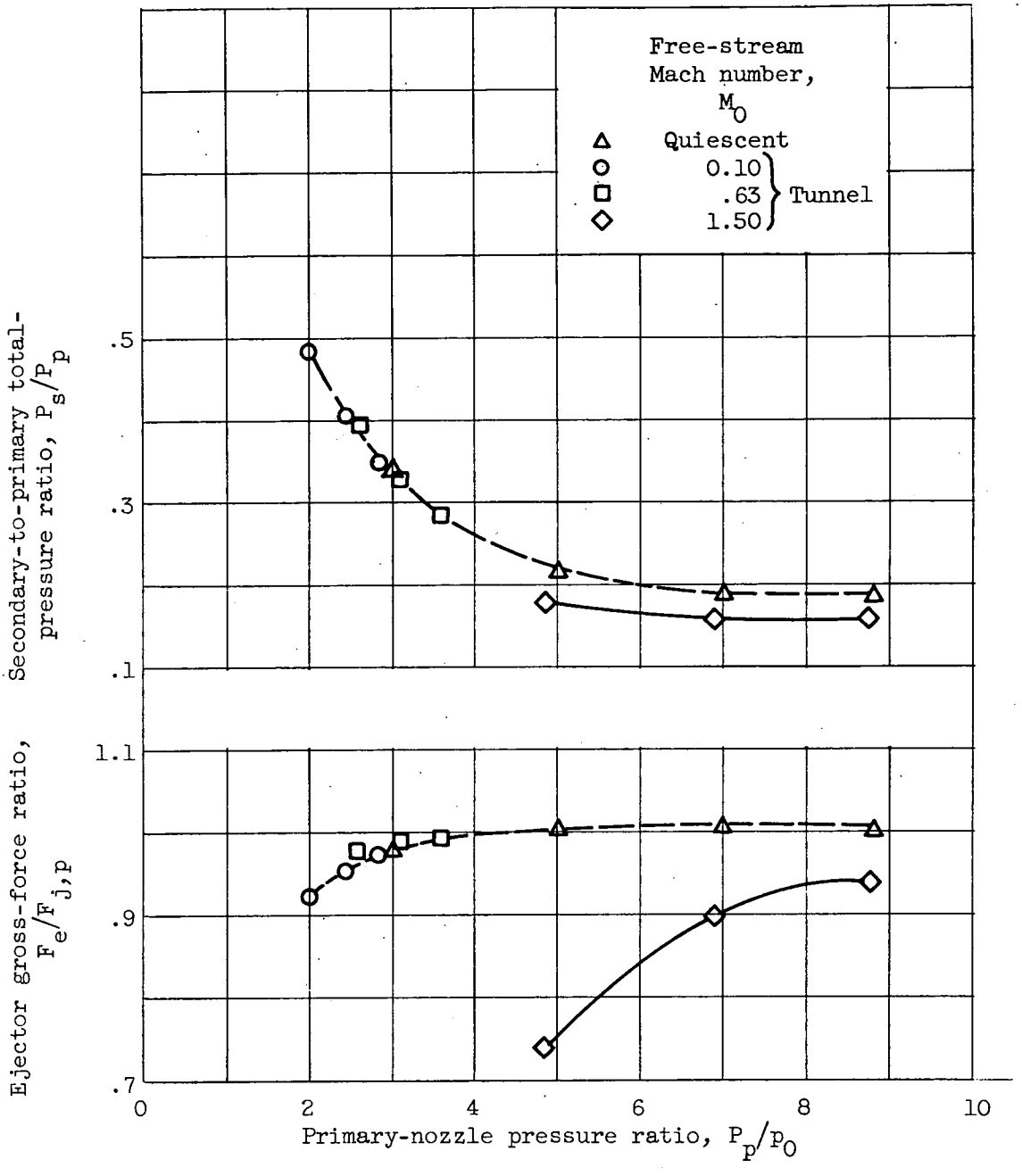

(b) Ejector 1.54-0.55.

Figure 13. - Continued. Comparison of quiescent-air and tunnel experimental data. Corrected weight-flow ratio, 0.05.

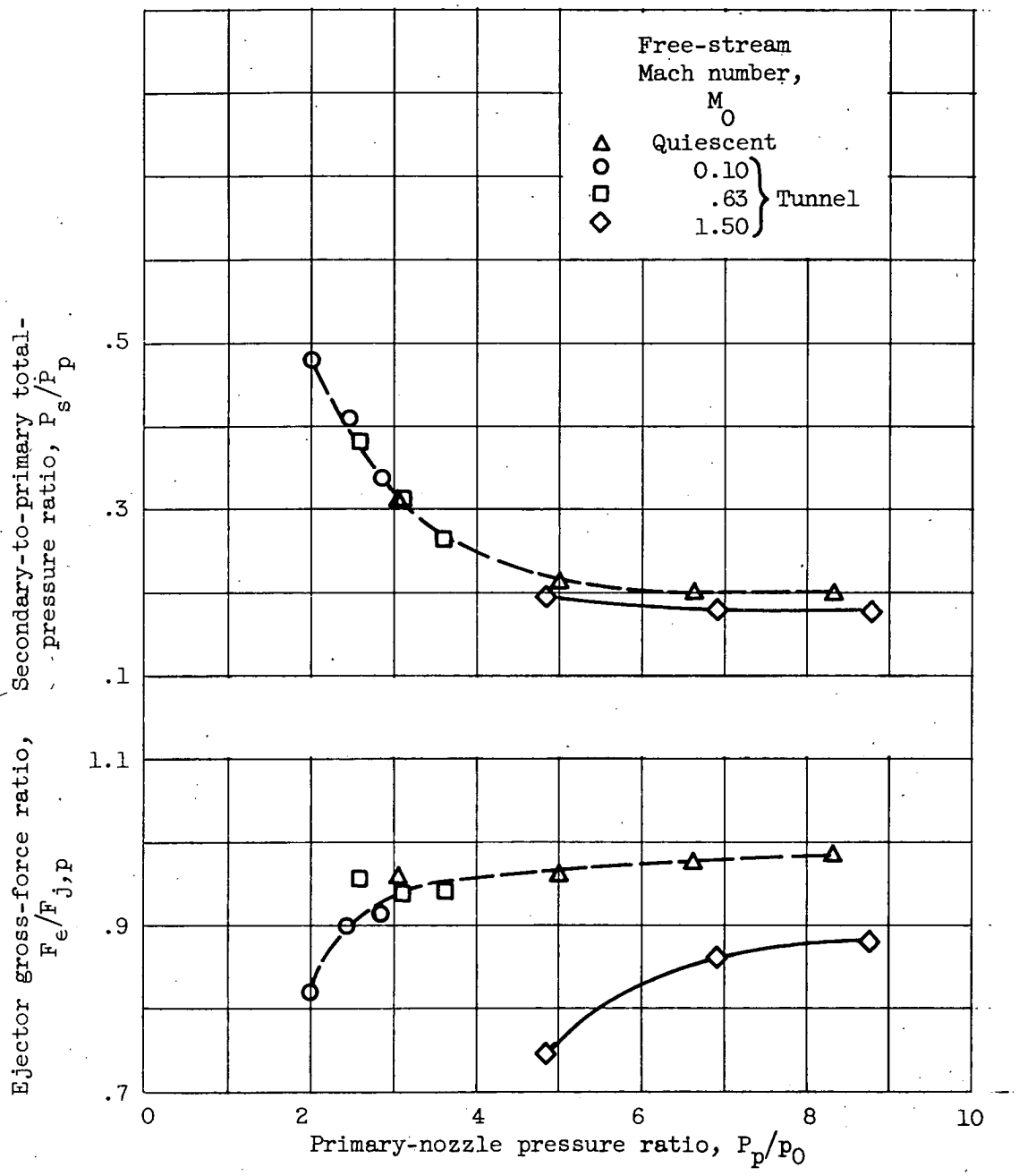

(c) Ejector 1.54-1.11S.

Figure 13. - Concluded. Comparison of quiescent-air and tunnel experimental data. Corrected weight-flow ratio, 0.05.

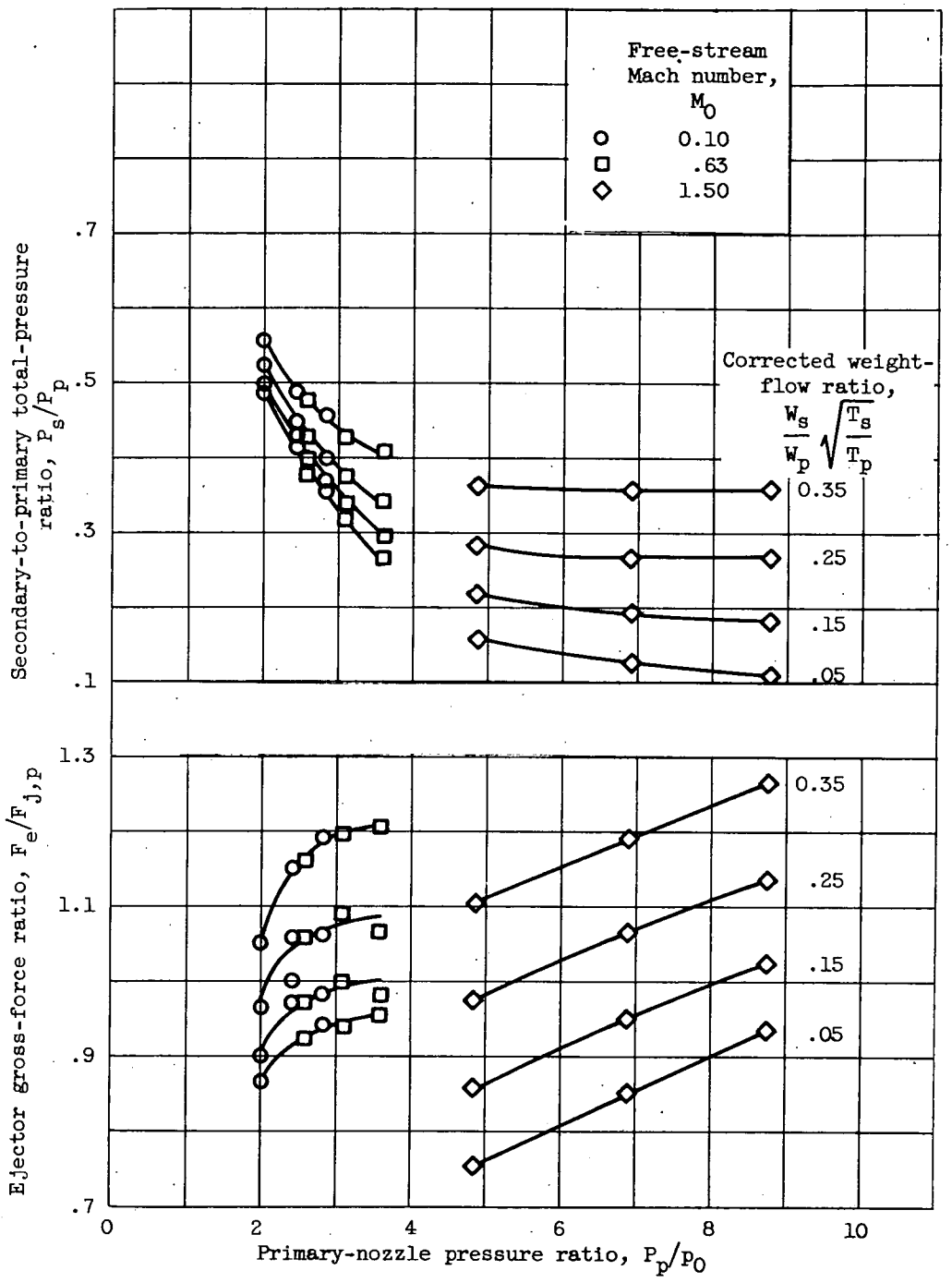

(a) Ejector 1.97-0.

Figure 14. - Effect of primary-nozzle pressure ratio and free-stream Mach number on ejector gross-force ratio and pumping characteristics.

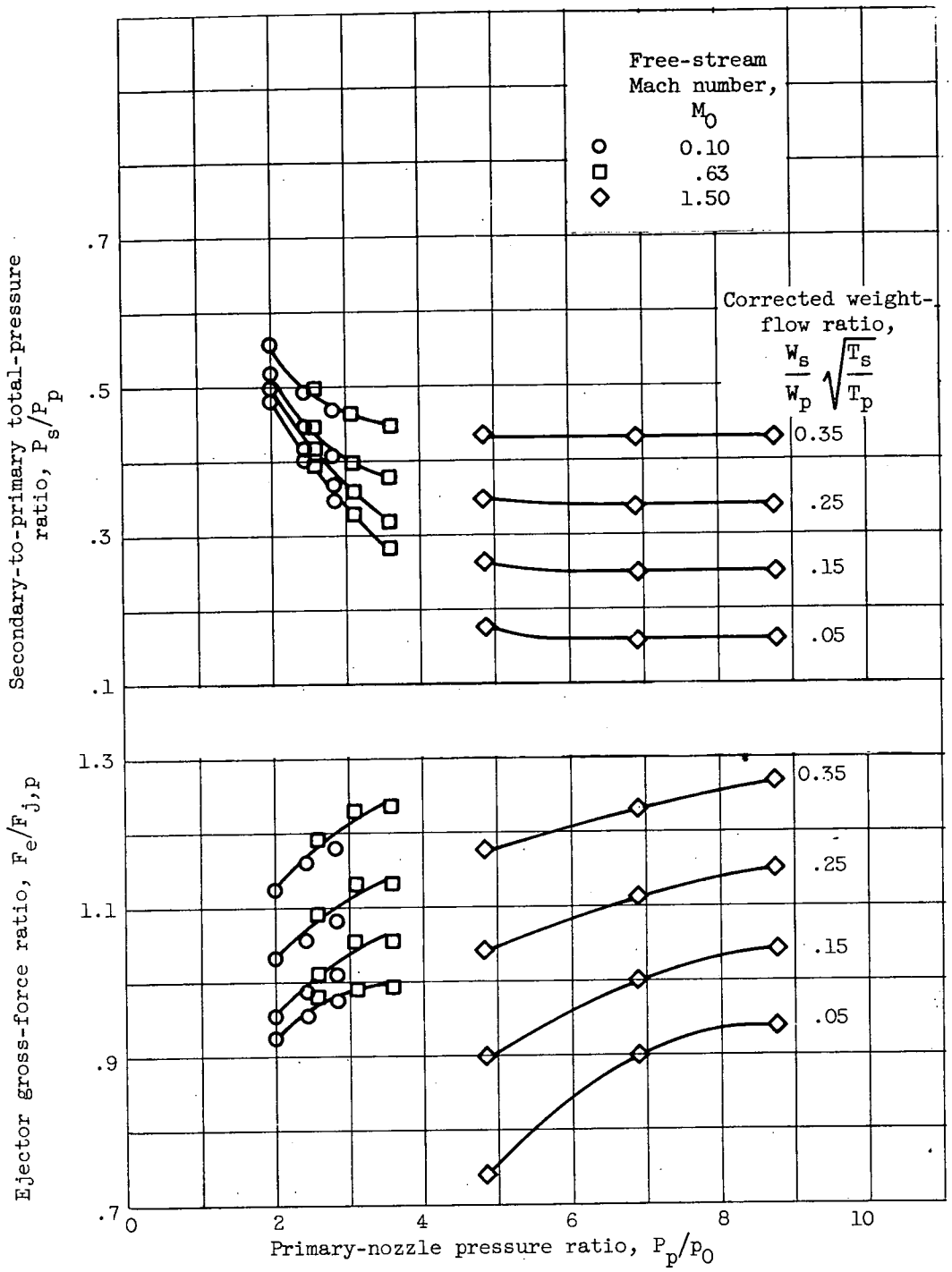

(b) Ejector 1.54-0.55.

Figure 14. - Continued. Effect of primary-nozzle pressure ratio and free-stream Mach number on ejector gross-force ratio and pumping characteristics.

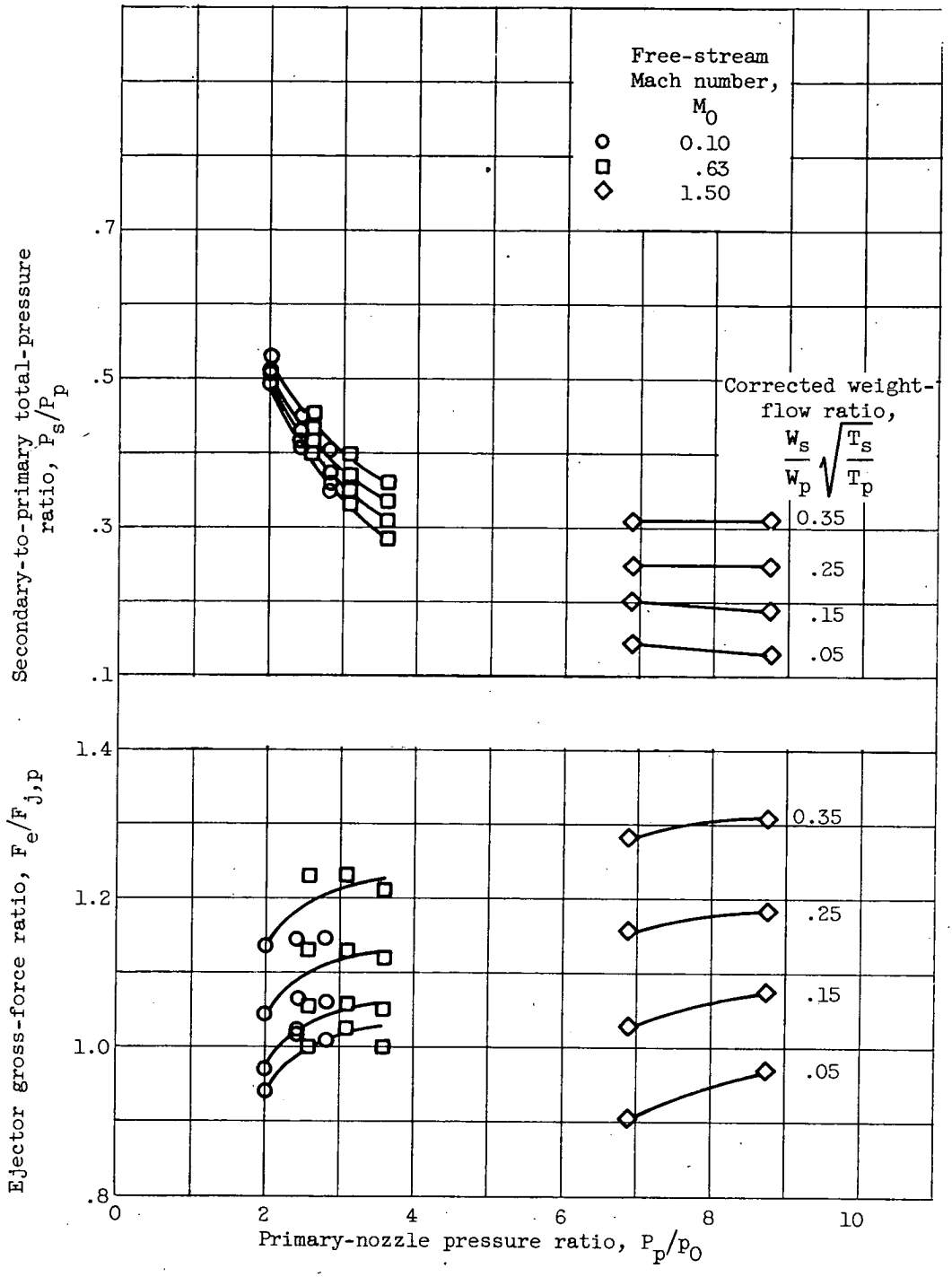

(c) Ejector 1.72-0.76.

Figure 14. - Continued. Effect of primary-nozzle pressure ratio and free-stream Mach number on ejector gross-force ratio and pumping characteristics.

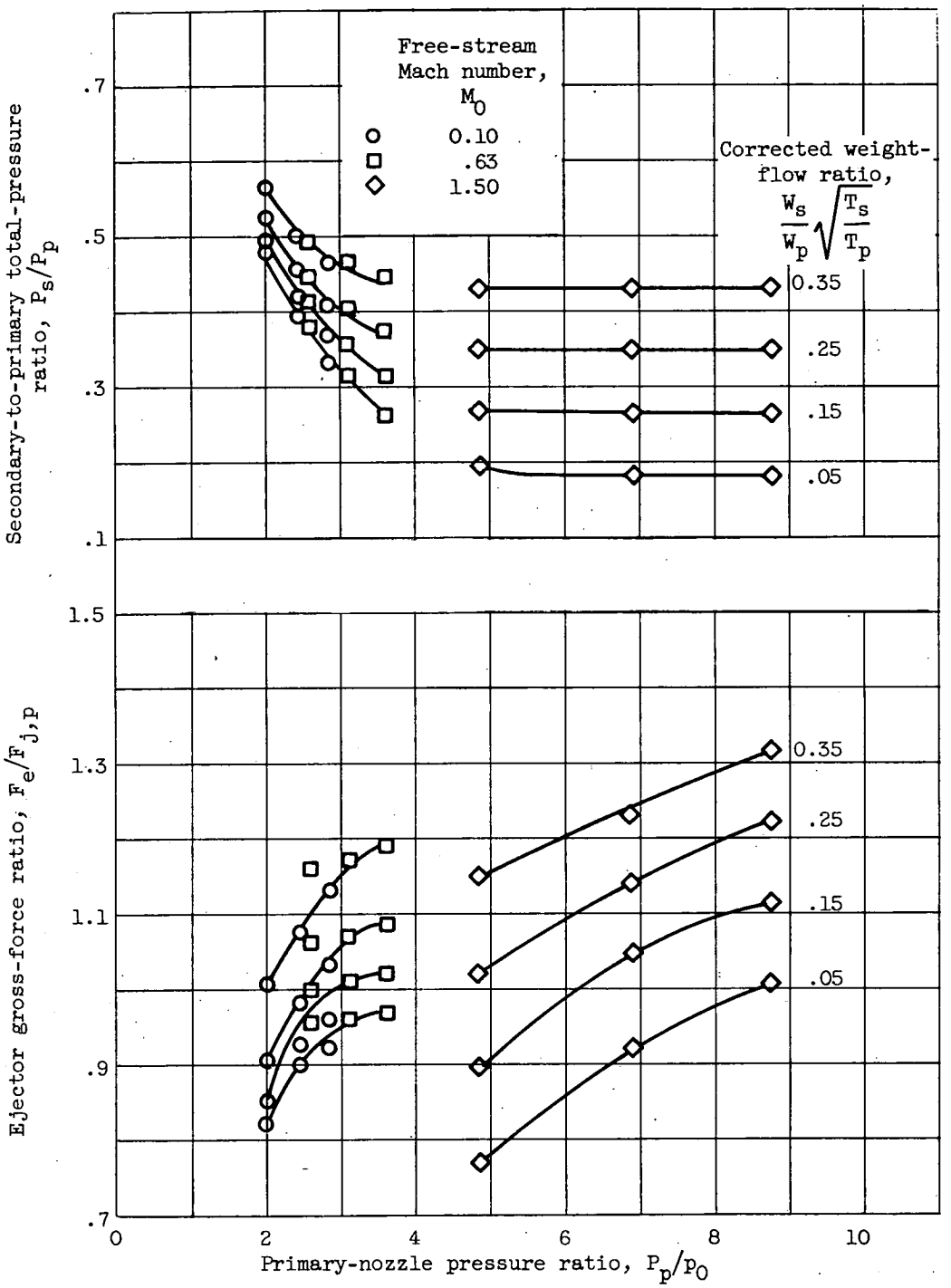

(d) Ejector 1.54-1.11.

Figure 14. - Continued. Effect of primary-nozzle pressure ratio and free-stream Mach number on ejector gross-force ratio and pumping characteristics.

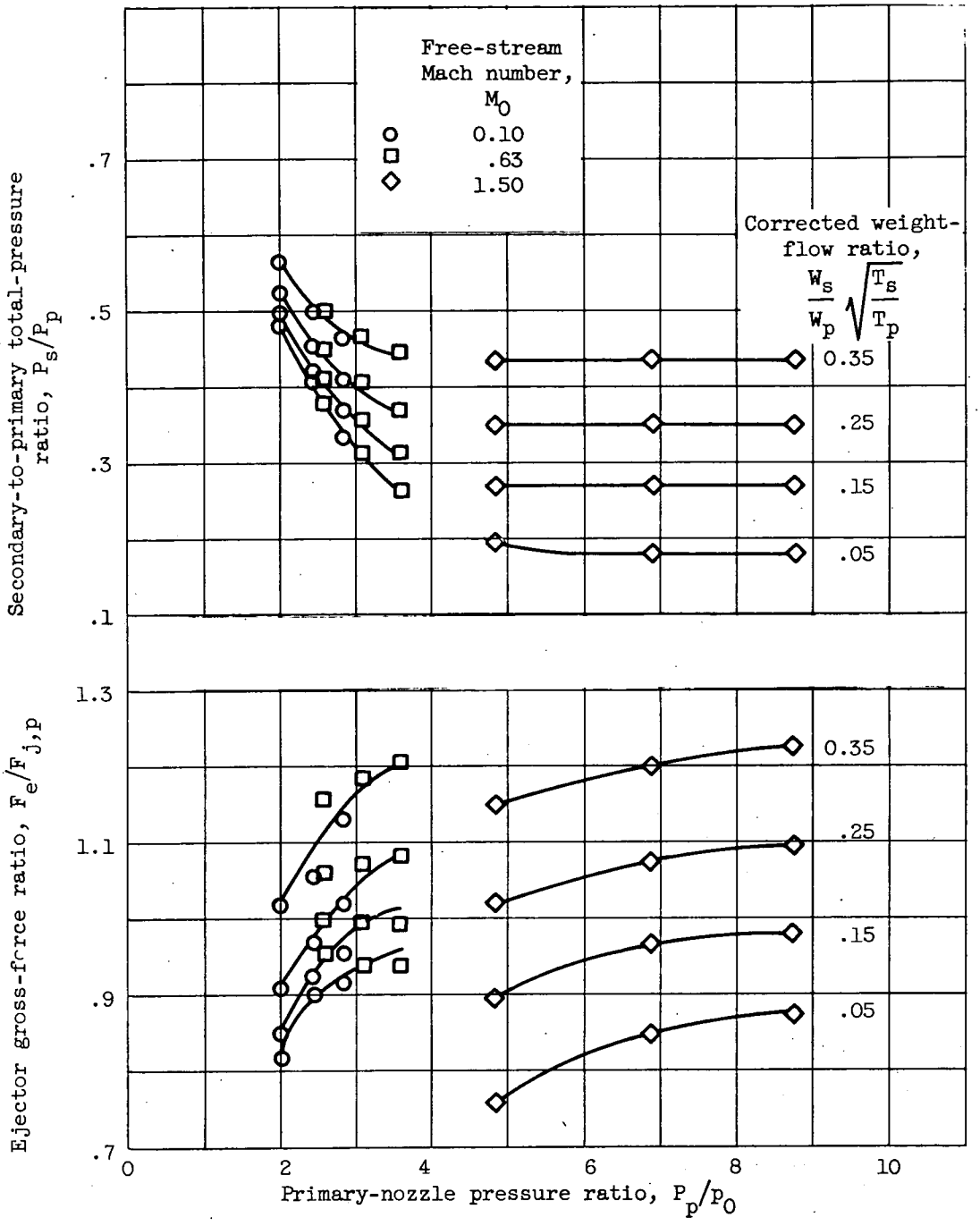

(e) Ejector 1.54-1.118.

Figure 14. - Concluded. Effect of primary-nozzle pressure ratio and free-stream Mach number on ejector gross-force ratio and pumping characteristics.

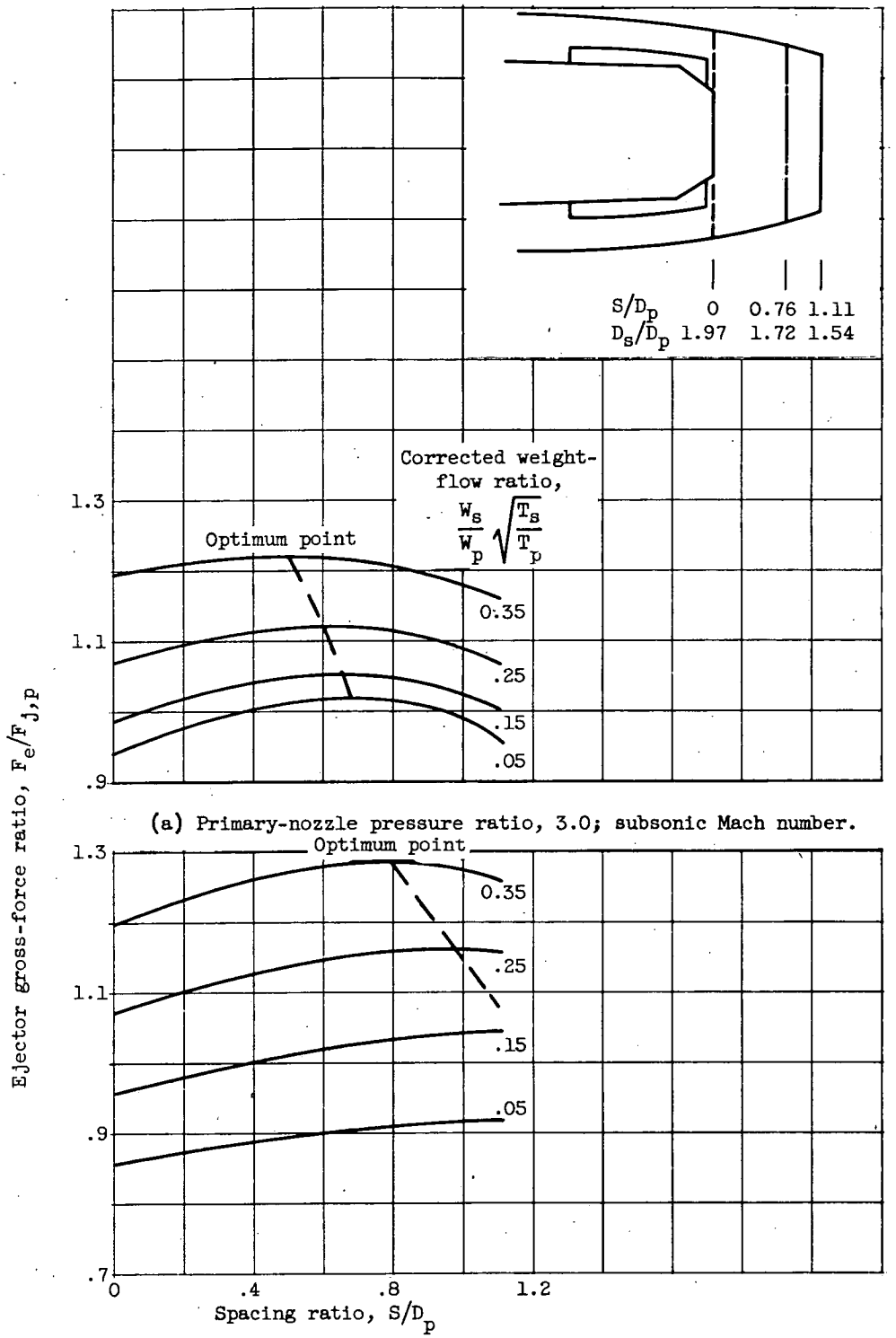

(a) Primary-nozzle pressure ratio, 3.0; subsonic Mach number.

(b) Primary-nozzle pressure ratio, 7.0; Mach number, 1.5.

Figure 15. - Effect of shroud length on ejector gross-force ratio.

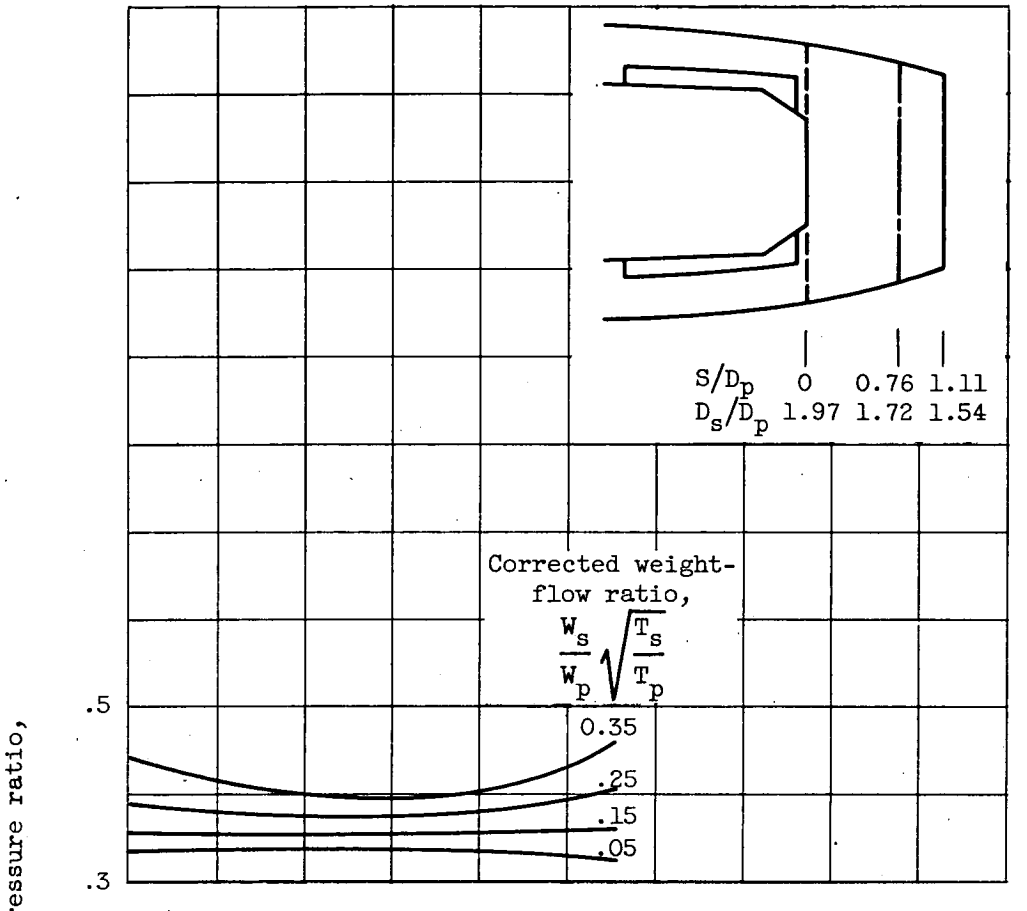

(a) Primary-nozzle pressure ratio, 3.0; subsonic Mach number.

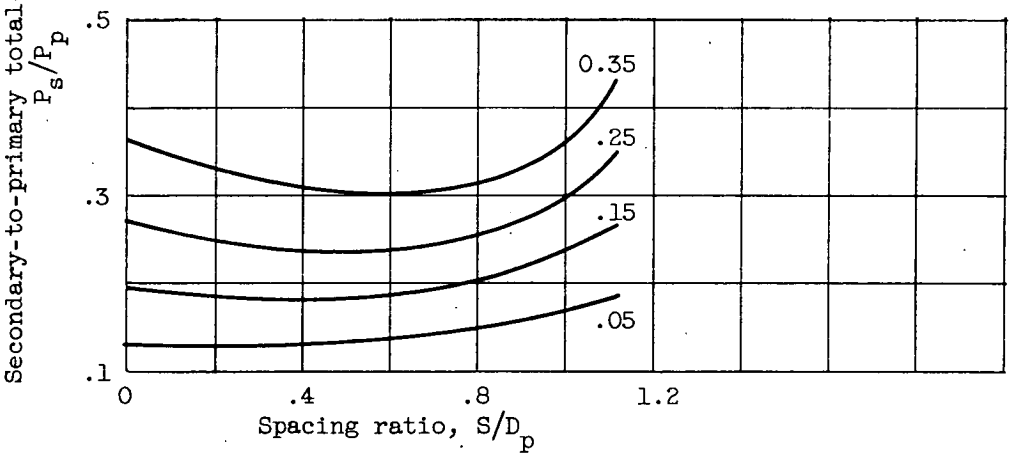

(b) Primary-nozzle pressure ratio, 7.0; Mach number, 1.5.

Figure 16. - Effect of shroud length on ejector pumping characteristics.

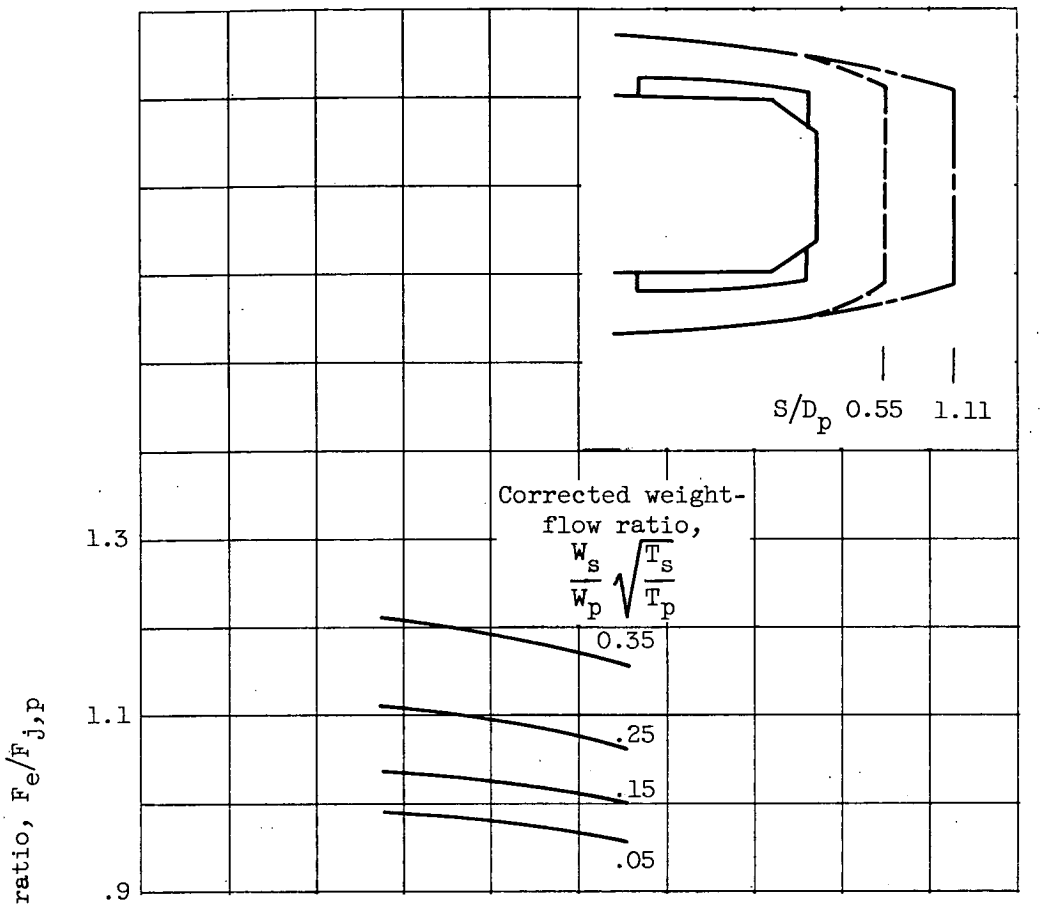

(a) Primary-nozzle pressure ratio, 3.0; subsonic Mach number.

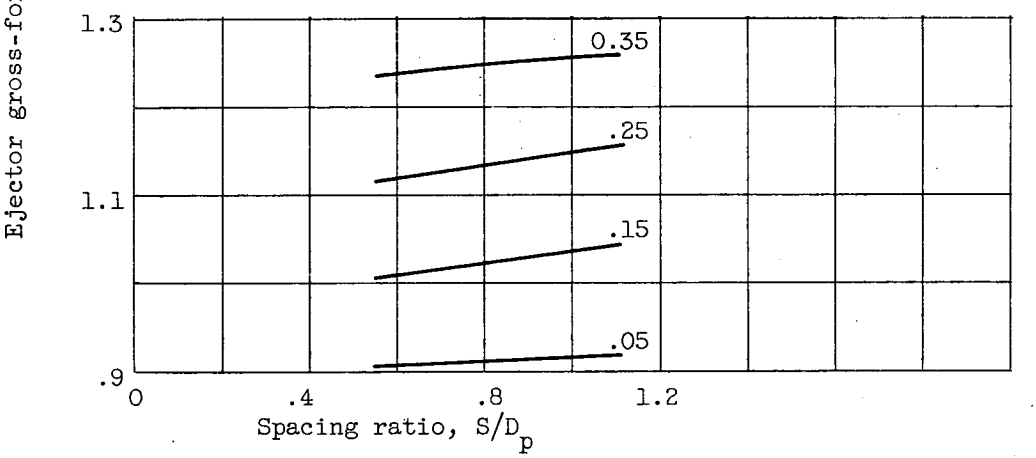

(b) Primary-nozzle pressure ratio, 7.0; Mach number, 1.5.

Ejector gross-force ratio, $F_e/F_{j,p}$

Figure 17. - Effect of spacing ratio on ejector gross-force ratio. Diameter ratio, 1.54.

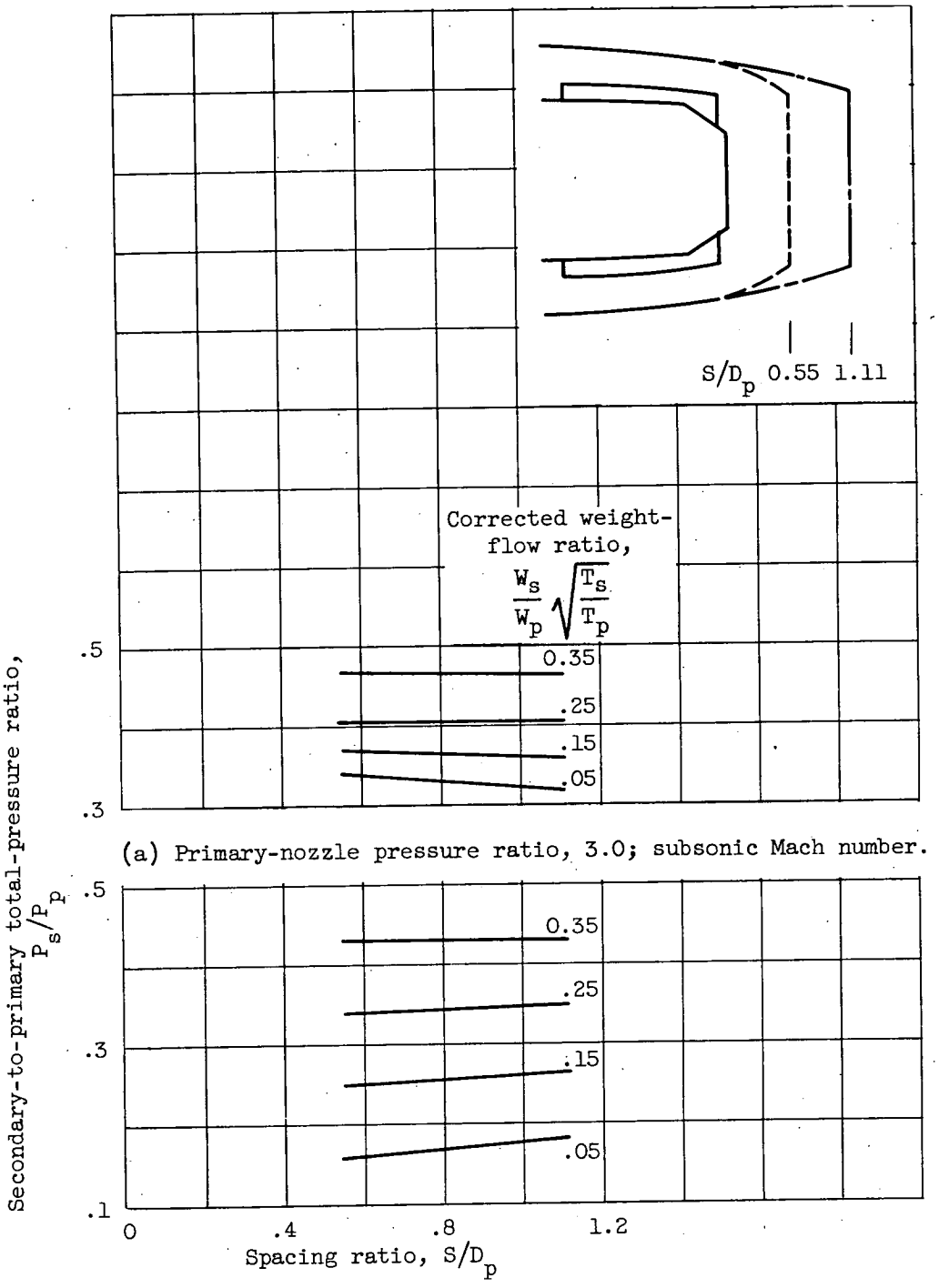

(a) Primary-nozzle pressure ratio, 3.0; subsonic Mach number.

(b) Primary-nozzle pressure ratio, 7.0; Mach number, 1.5.

Figure 18. - Effect of spacing ratio on ejector pumping characteristics. Diameter ratio, 1.54.